L14: Multifunctional Drug Delivery Systems

May 22, 2018

Multifunctional delivery systems

- **Dual Drug Delivery: Combination Therapy**

- **Theragnosis: Therapy and Diagnosis**

Combination Therapy

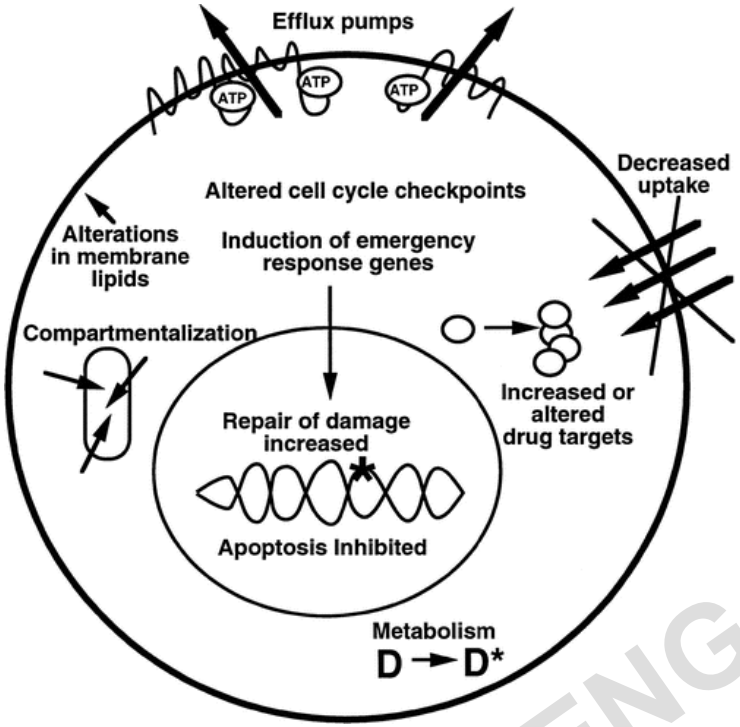

Cancer drug resistance:

- Adapted drug efflux pump
- Altered drug target
- Increased drug metabolism

Combination drug therapy:

- Generate synergies among different drugs
- Slow the development of drug resistance
- Reduce treatment failure rate
- Reduce case-fatality ratios
- Reduce the need to develop new drugs

Cocktail vs. Co-delivery

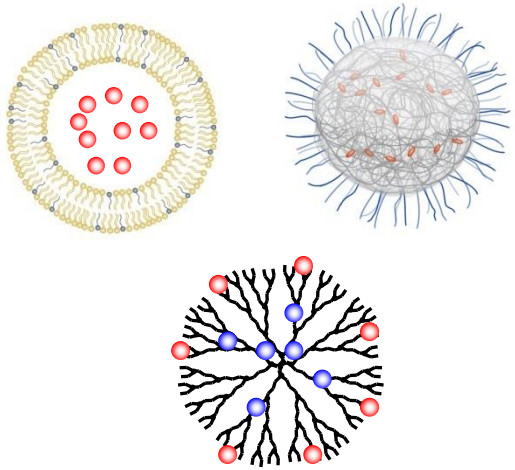

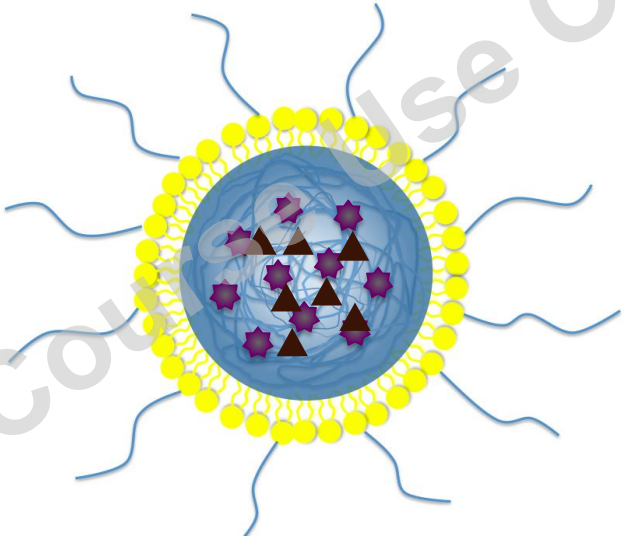

Cocktail administration:

- Varying pharmacokinetics
- Varying biodistribution
- Varying membrane transport
- Difficult dosing and scheduling optimization

Co-delivery:

- Unified pharmacokinetics
- Ratiometric drug loading
- Temporal drug release

Dual Drug Delivery – Example 1

Step-by-step in fighting cancer!

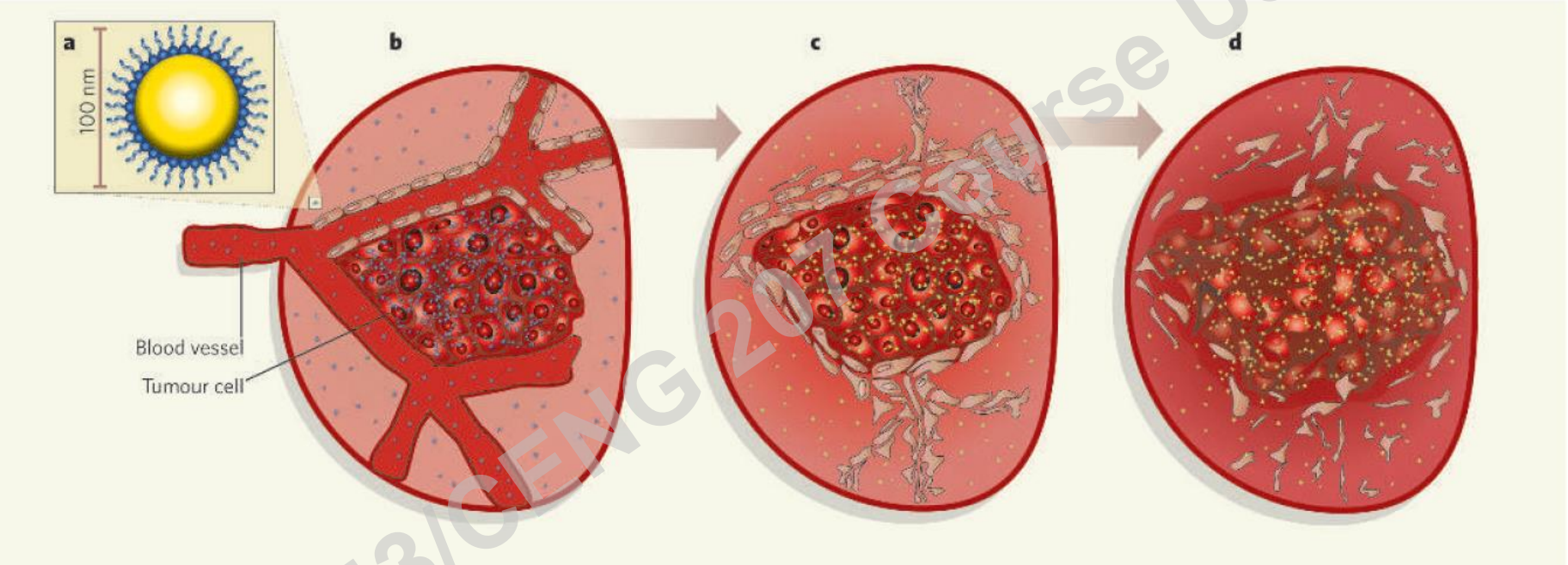

Traditional chemotherapy kills tumour cells directly; some newer drugs work instead by cutting the tumour's blood supply. An innovative approach combines these strategies sequentially to pack a double whammy.

Nanocell Synthesis and Characterization

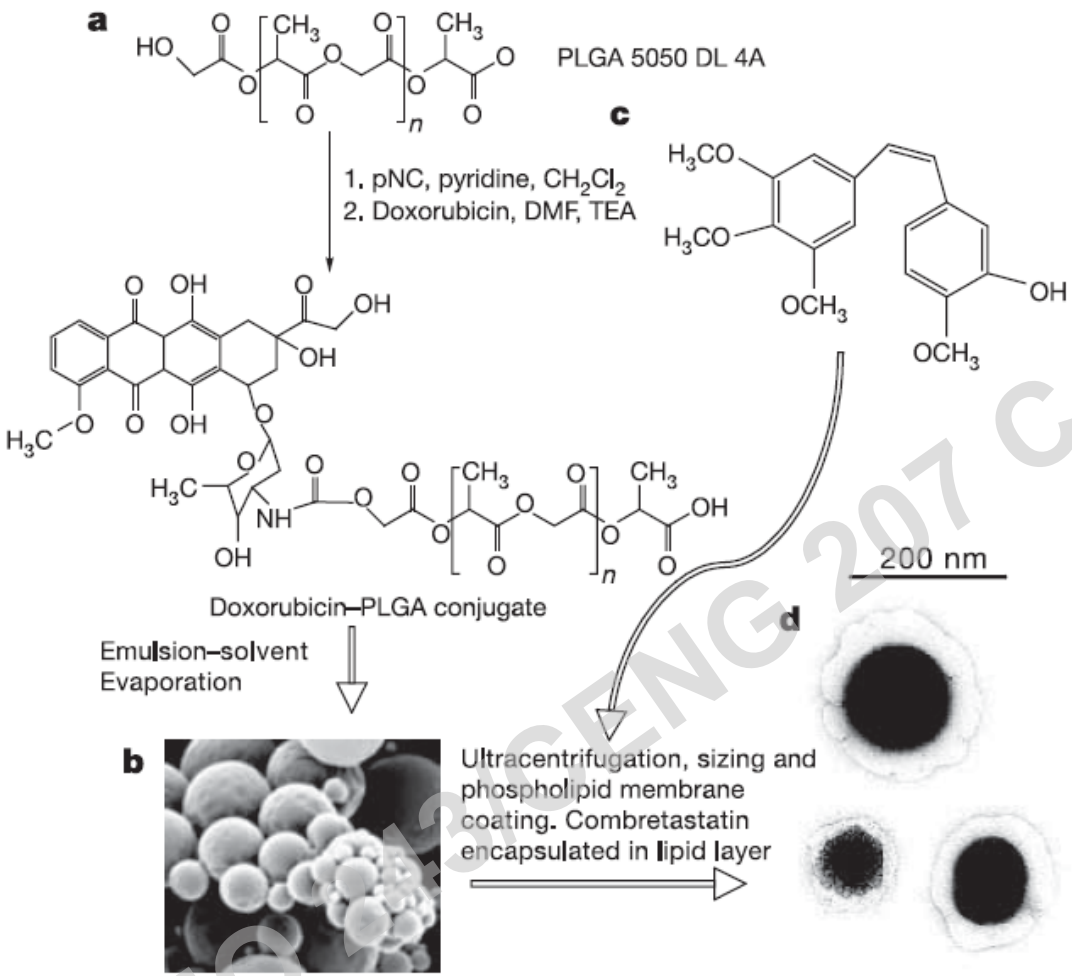

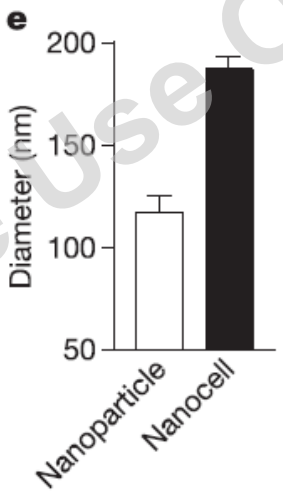

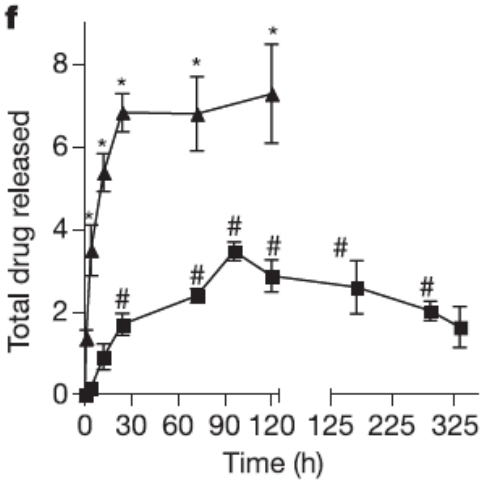

Nature, ***2005***, *436*, 568-572

3D Co-culture *In Vitro* Bioassay

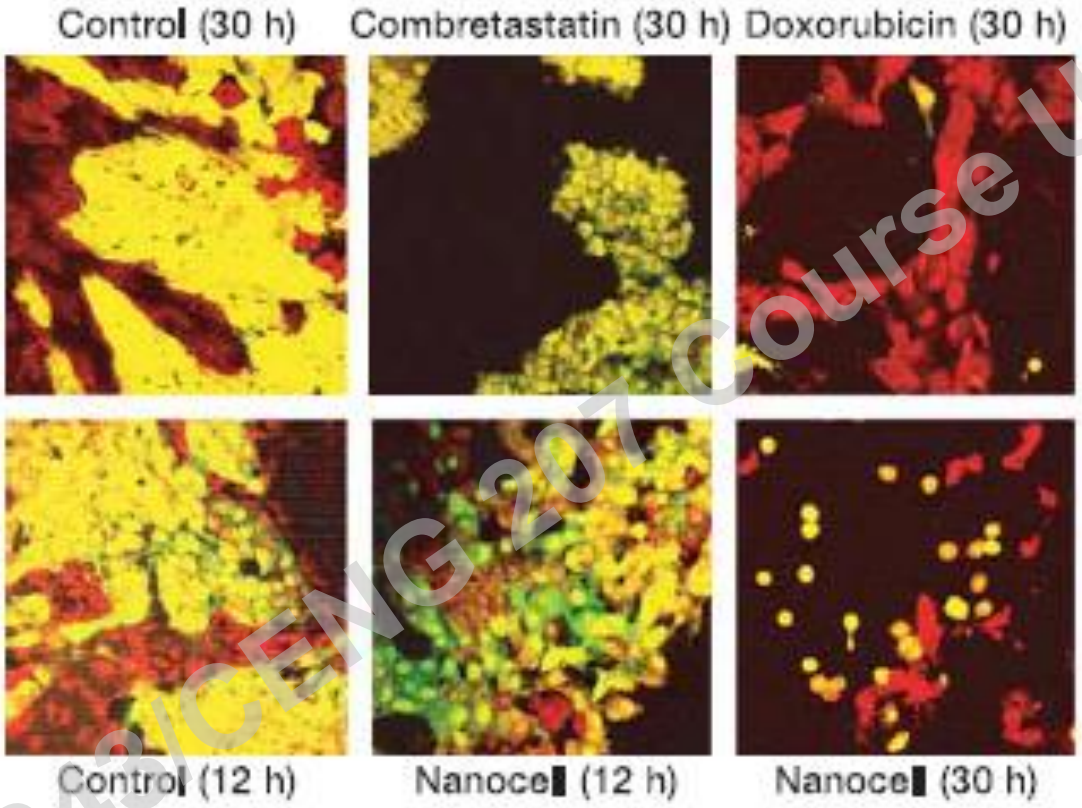

Co-culture: Melanoma (yellow) + Endothelium (red)

Nanocells Inhibit Tumor Growth

Lewis lung carcinorma **Melanoma**

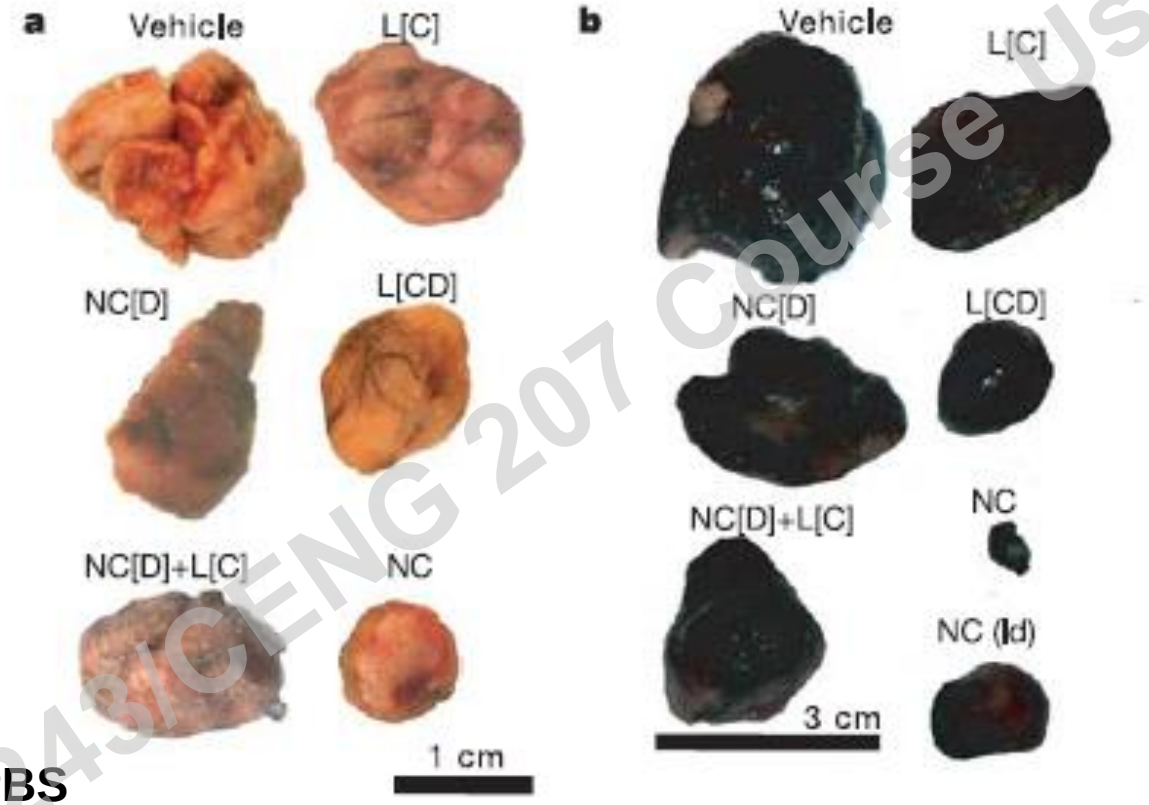

Vehicle: PBS
NC[D]: nanocells containing only doxorubicin
L[C]: combretastatin-encapsulated liposomes
NC[D]+L[C]: co-administration of NC[D]+L[C]
NC: nanocells containing both doxorubicin and combretastatin
L[CD]: liposomes cotaining both doxorubicin and combretastain

Nanocells Inhibit Tumor Growth

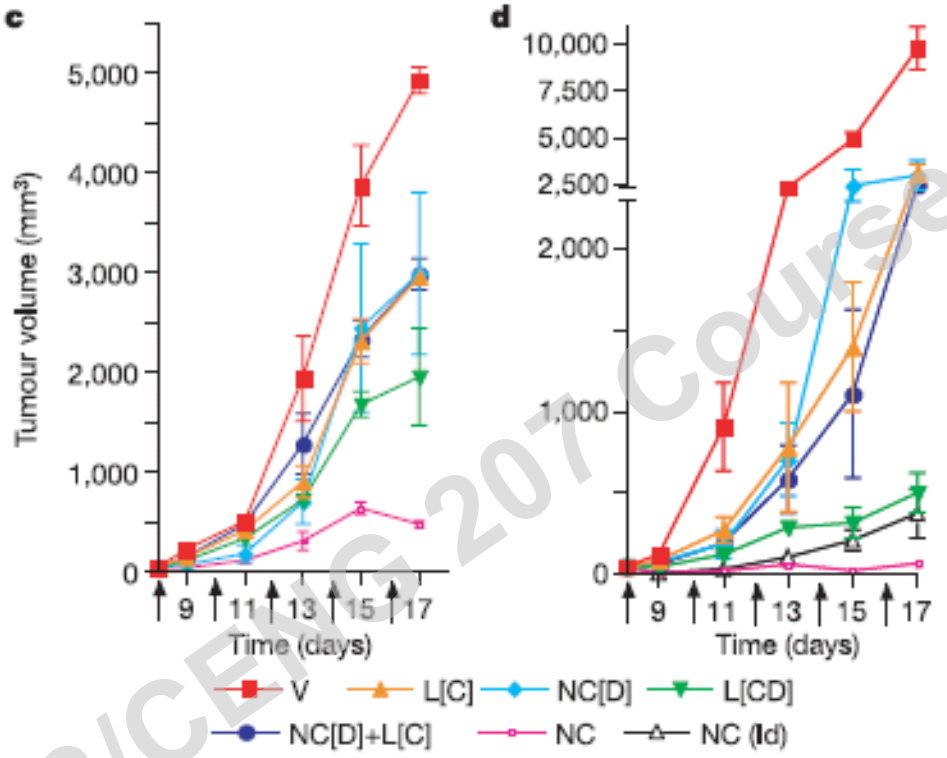

Tumour volume in different treatment groups for Lewis lung carcinoma (**c**) and B16/F10 carcinoma (**d**).

Survival and Toxicity

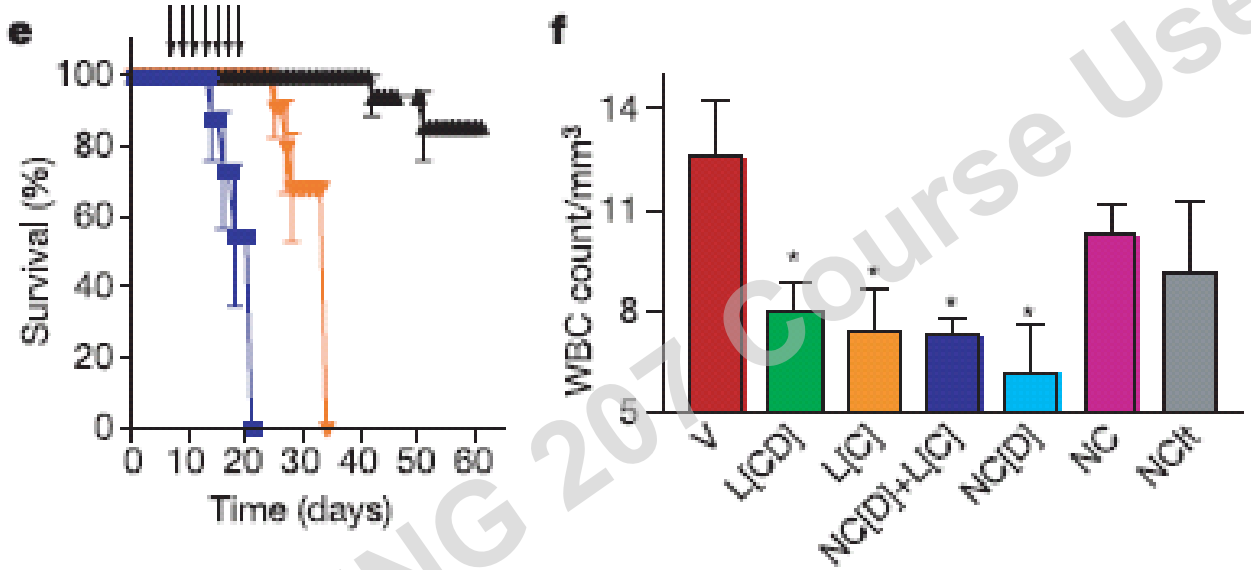

e, Survival graph showing that treatment with NC significantly increases the lifespan: blue squares, vehicle; black triangles, NC; orange triangles, L[CD].

f, The effect of different treatments on the white blood cell (WBC) counts

Dual Drug Delivery – Example 2

Combinatorial nanotherapeutics: Rewiring, then killing, cancer cells

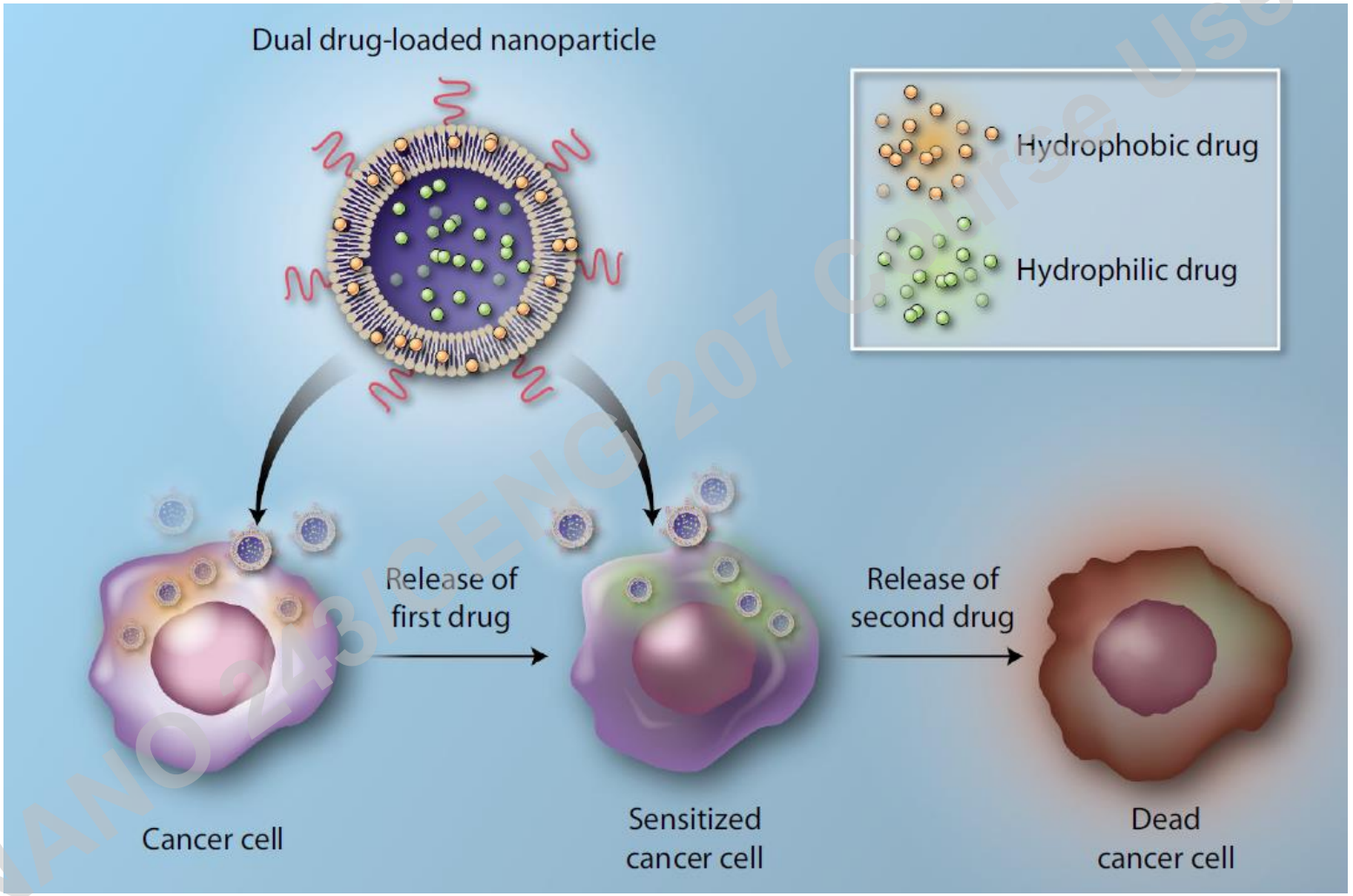

Science Signaling 2014, **7** (325), pe13

Dual-Drug-Loaded Liposomal System

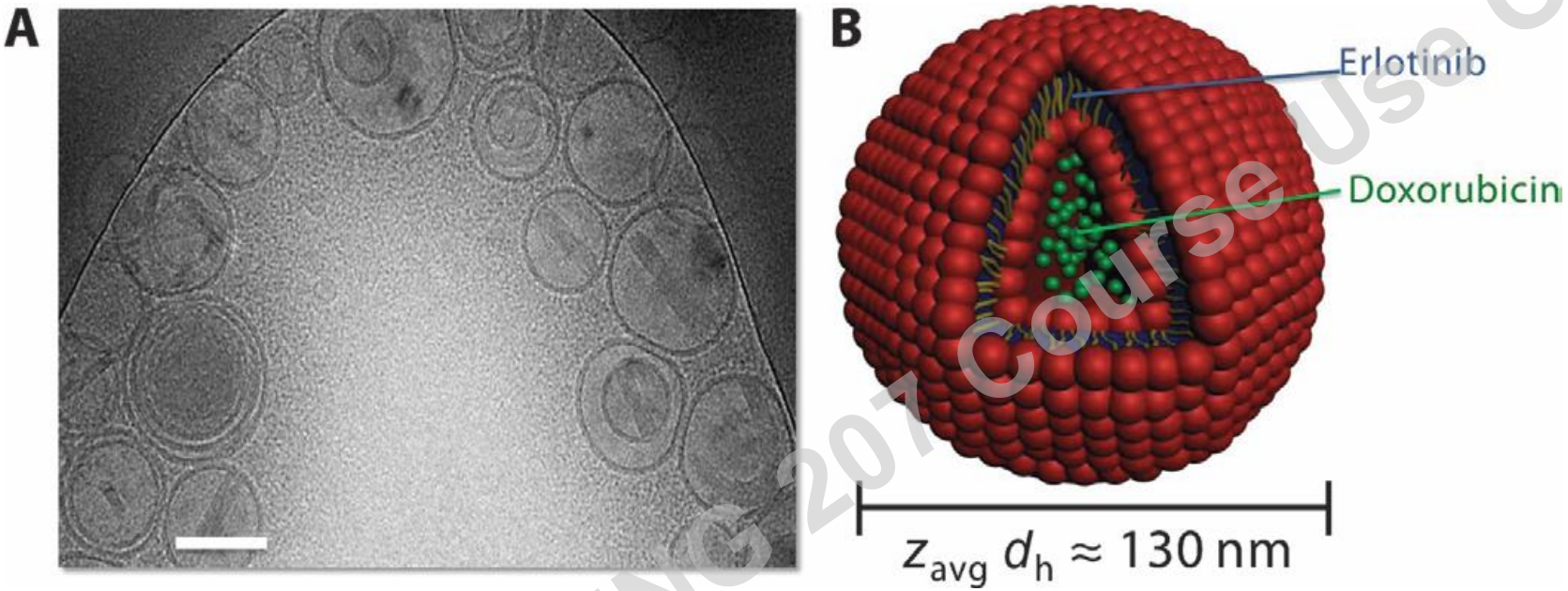

Characterization of the combination therapeutic–loaded liposomal system. (A) Cryogenic transmission electron micrograph of dual drug–loaded liposomes. Scale bar, 100 nm. (B) Schematic of dual loading of a small-molecule inhibitor (erlotinib, blue) into the hydrophobic, vesicular wall compartment and of a cytotoxic agent (doxorubicin, green) into the aqueous, hydrophilic interior.

Science Signaling 2014, **7** (325), ra44

Drug Release & Cytotoxicity

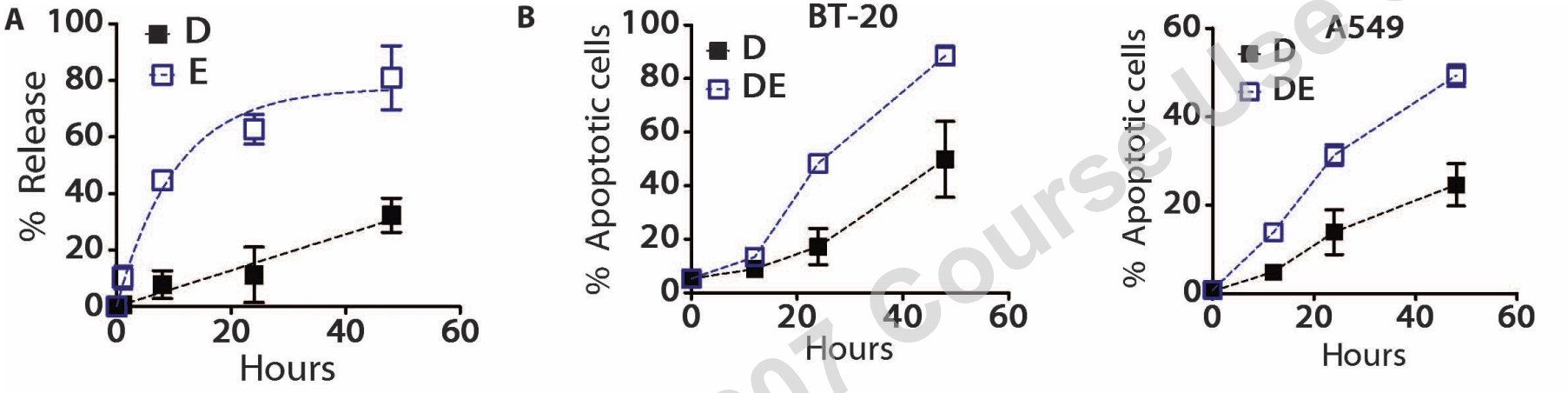

Evaluation of the dual drug–loaded liposomal system in vitro. (A) Drug release from dual drug–loaded liposomes in an excess volume of PBS (pH 7.4) at 37°C under agitation. (B) Comparative cytotoxicity of dual drug–loaded liposome relative to the single drug–loaded liposome in BT-20 (TNBC) and A549 (NSCLC) cell lines.

Functionalization for Targeted Delivery

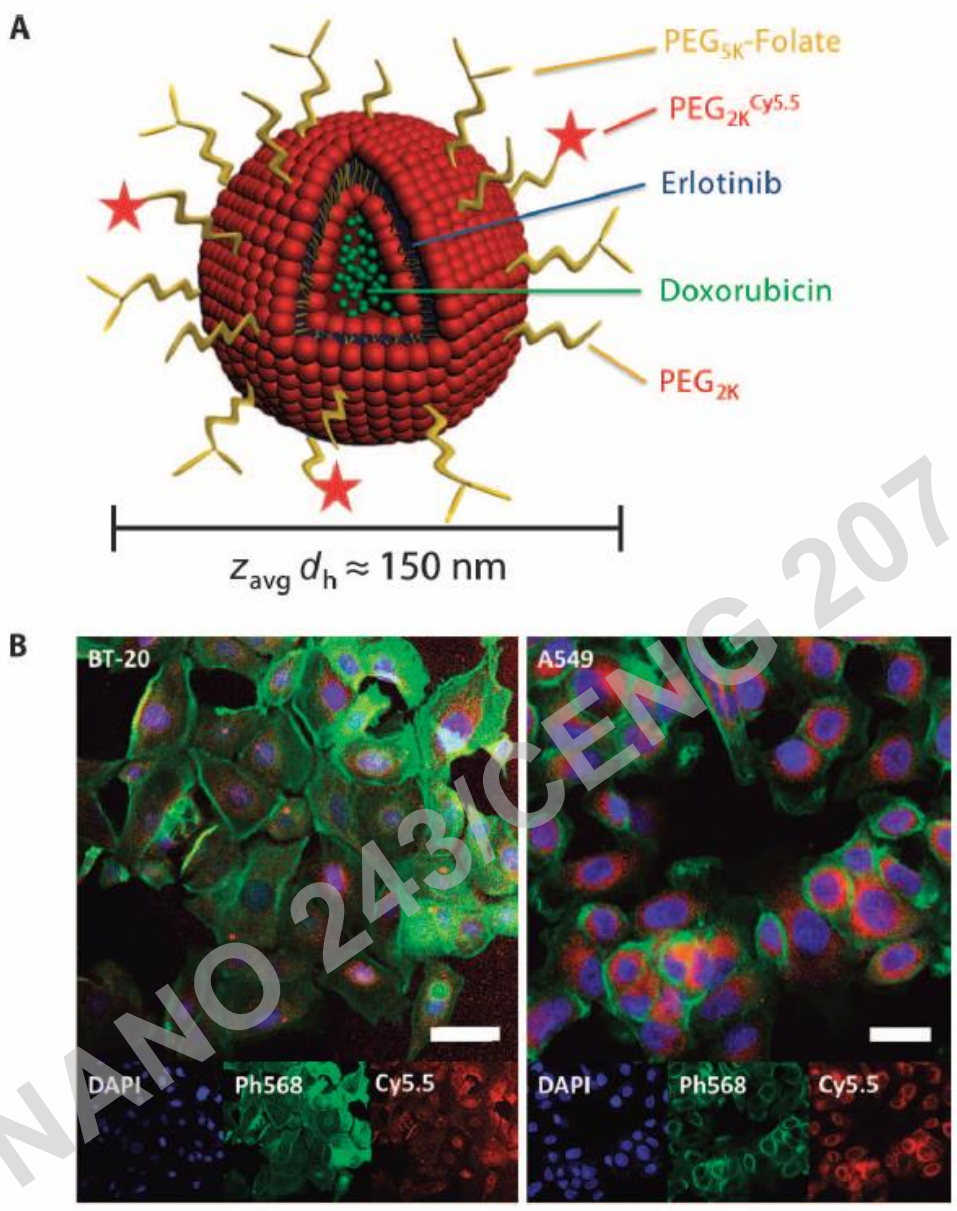

(A) Schematic of addition of DSPE-PEG2K (0.5 mol % ratio) to minimize nonspecific protein binding, DSPE-PEG2K Cy5.5 (0.1 mol % ratio) for fluorescent tracking, and DSPE-PEG5K-folate (0.5 mol % ratio) for cell targeted delivery. (B) Cell uptake of the folate-targeted liposomes in BT-20 and A549 cells, visualized by confocal microscopy. Blue, nuclei labeled with DAPI; green, actin labeled with phalloidin-568 (Ph568); red, DSPE-PEG2K Cy5.5–labeled DFP liposomes. Bottom panels represent the fluorescence in each channel; top panels are merged images.

Anticancer Efficacy against NSCLC Model

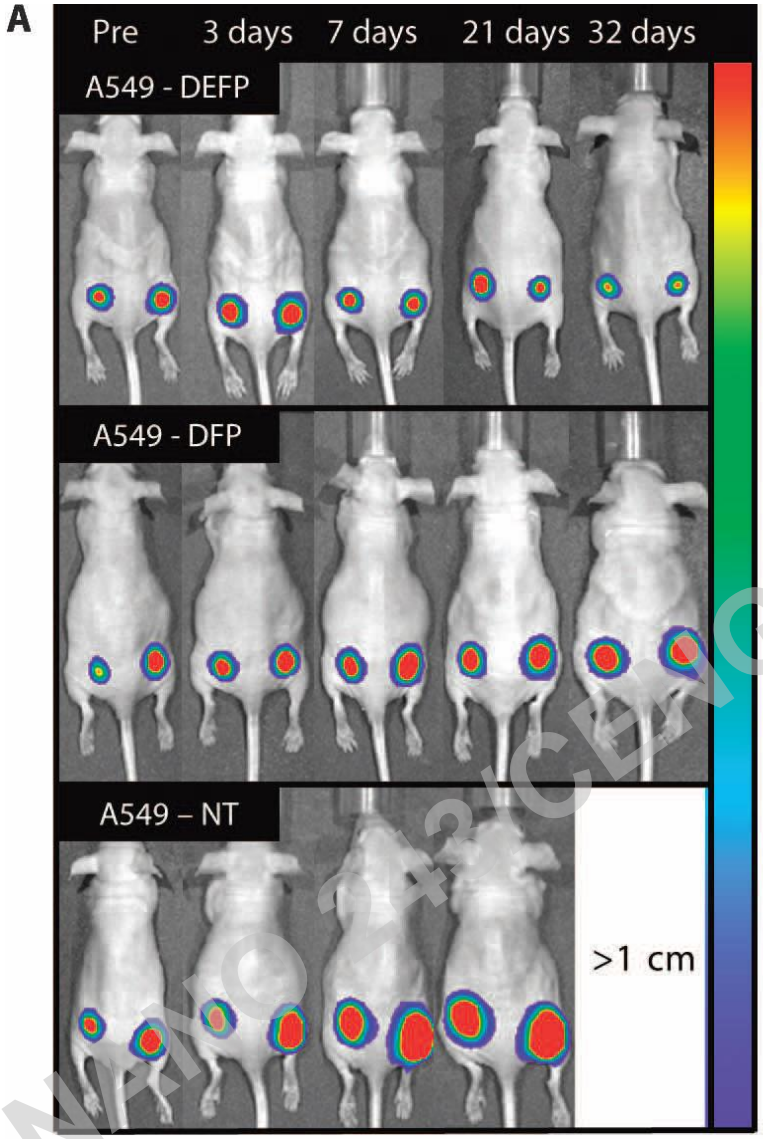

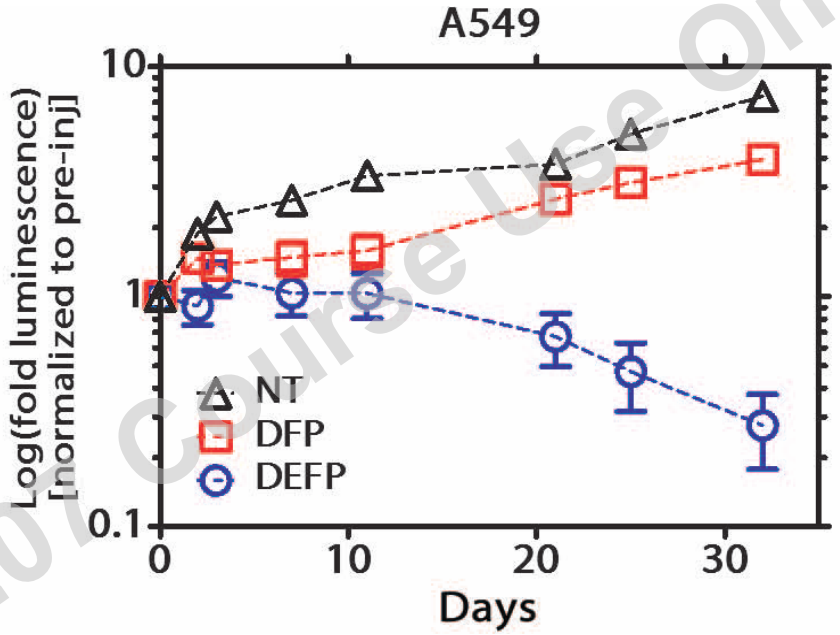

A549-luciferase–expressing, NSCLC xenograft-bearing NCR nude mice. Tumor-imaging data for dual drug (DEFP, top), single drug (DFP, middle), and untreated control, along with luminescence quantification (reported as fold initial tumor luminescence, presented on a semi-log plot) corresponding to tumor size as a function of time, after a single administration of drug (1 mg/kg)–loaded liposomal formulations.

Anticancer Efficacy against NSCLC Model

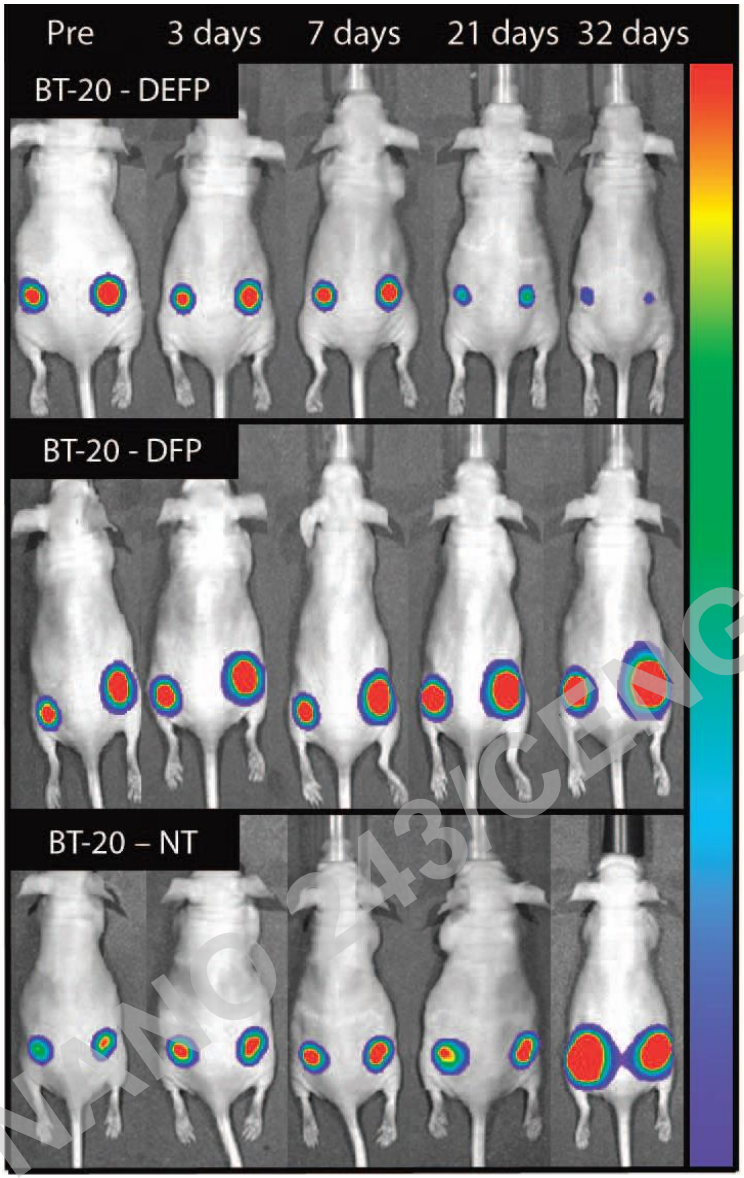

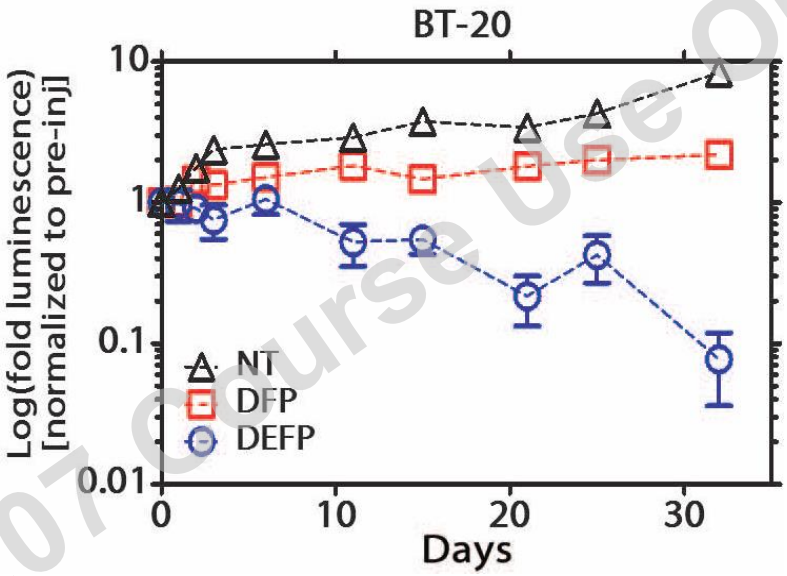

BT-20-luciferase–expressing, TNBC xenograft-bearing NCR nude mice. Tumor-imaging data for dual drug (DEFP, top), single drug (DFP, middle), and untreated control, along with luminescence quantification (reported as fold initial tumor luminescence, presented on a semi-log plot) corresponding to tumor size as a function of time, after a single administration of drug (1 mg/kg)–loaded liposomal formulations.

Dual Drug Delivery – Example 3

Drug A-Polymer

Drug B-Polymer

Drug A/Drug B with a desirable molar ratio

DOX-PLA

CPT-PLA

Lipid

PEG

Self assembly

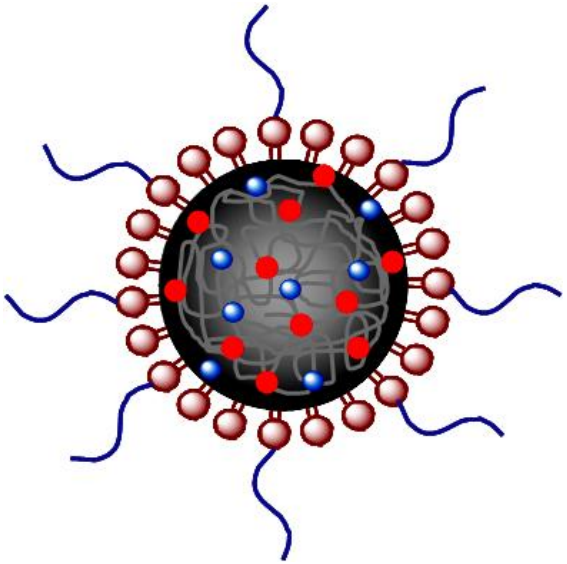

*Mol. Pharm. 2011, **8**, 1401*

Synthesis of DOX-PLA and CPT-PLA Conjugates

DOX-PLA

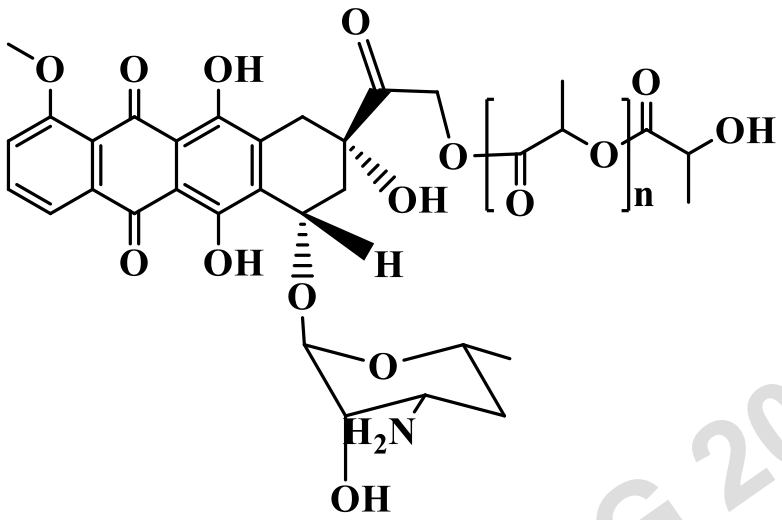

CPT-PLA

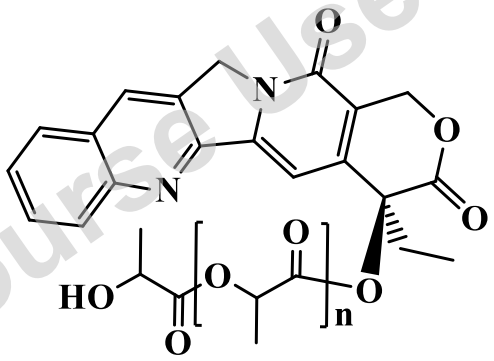

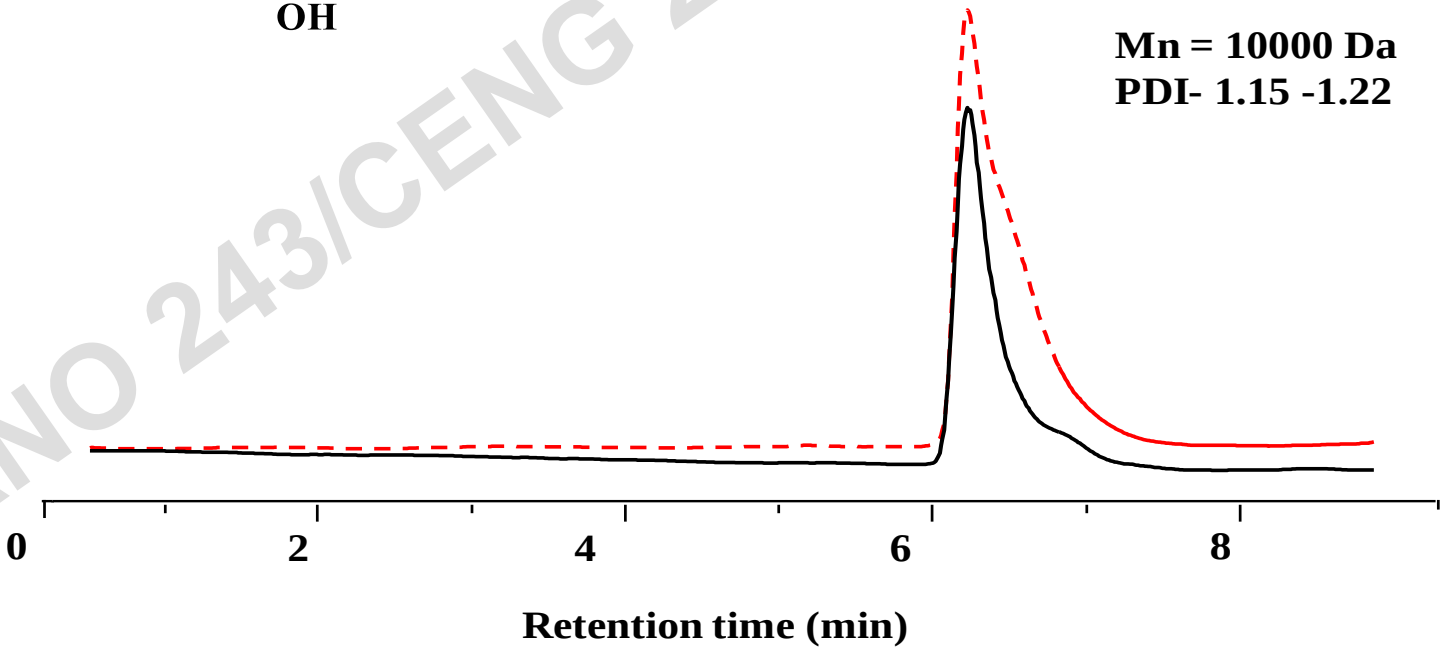

DOX-PLA/CPT-PLA Nanoparticles

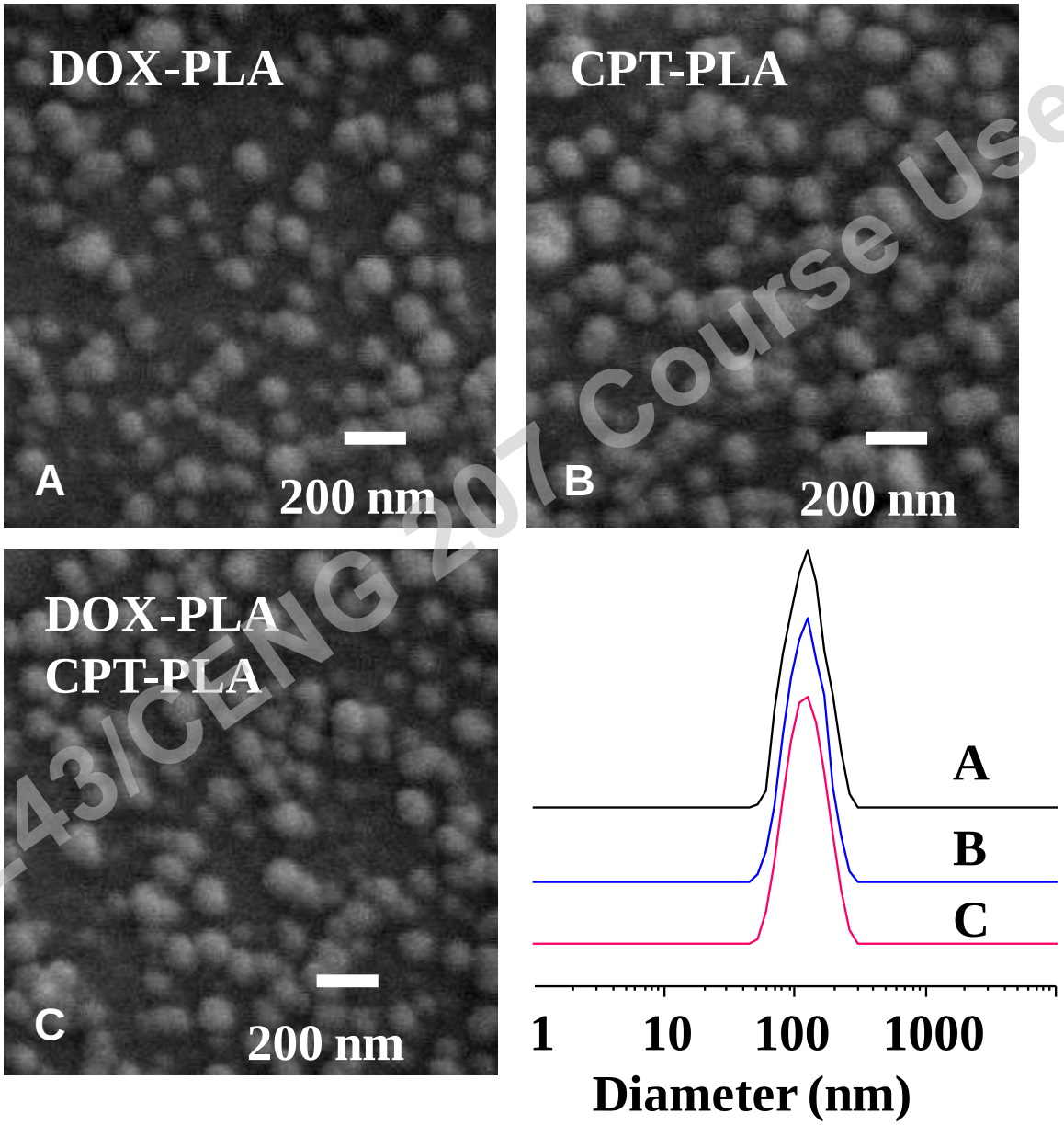

Ratiometric Loading of DOX and CPT

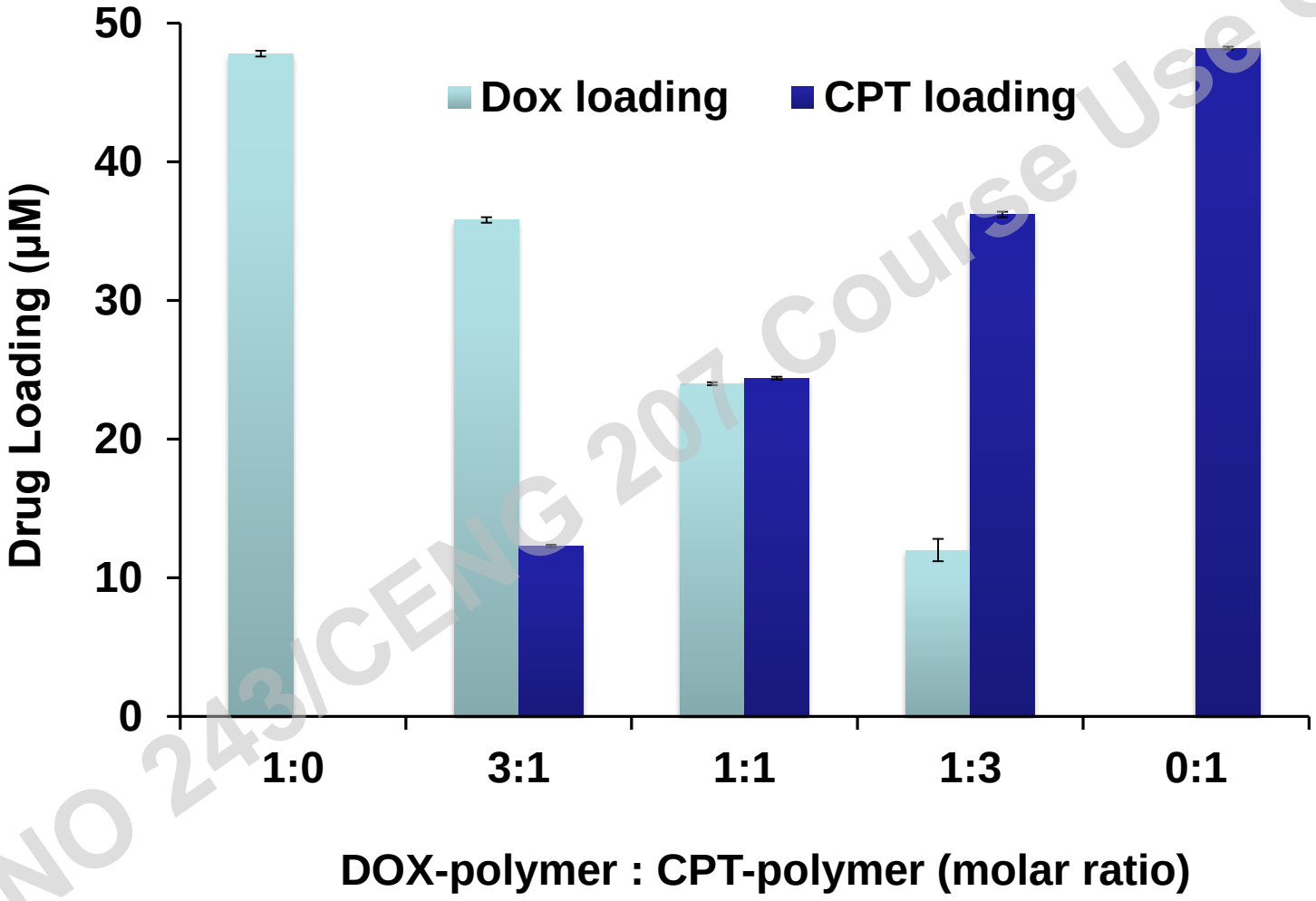

Co-delivery of DOX and CPT

MDB-MB-435 breast cancer cell

Synergistic Toxicity against Breast Cancer Cells

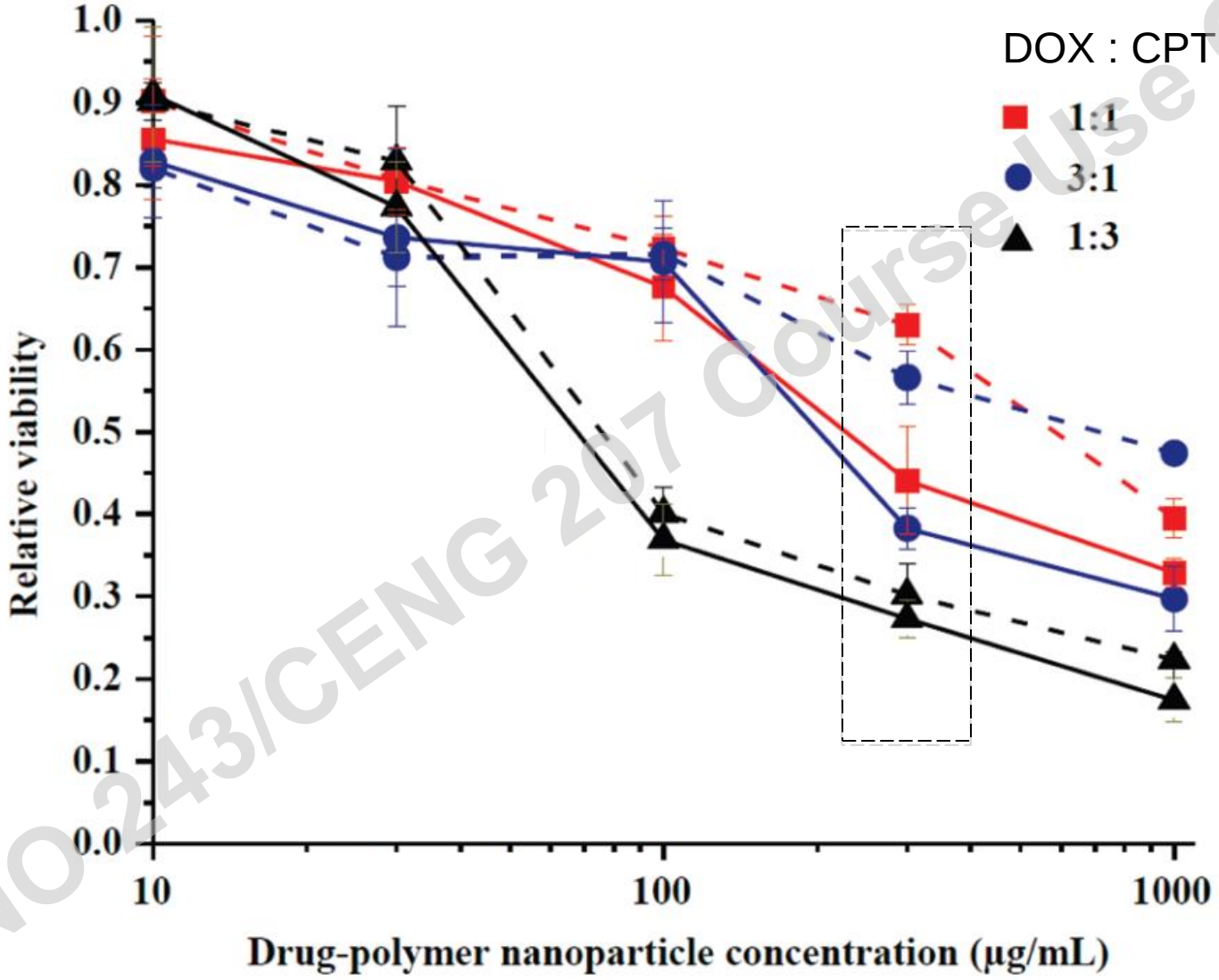

Theranostics

Therapeutics + Diagnostics at the same time

Real time, non-invasive
In vivo images on therapy
Drug screening and mechanistic studies

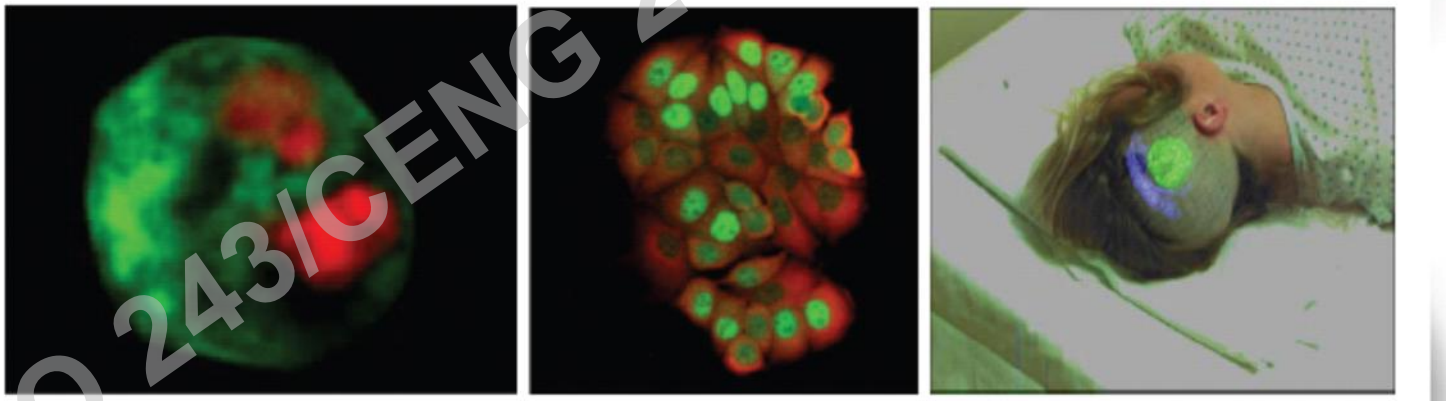

Theranostics – Example 1

Quantum dot-aptamer conjugates for synchronous cancer imaging, therapy, and sensing of drug delivery based on bi-fluorescence resonance energy transfer

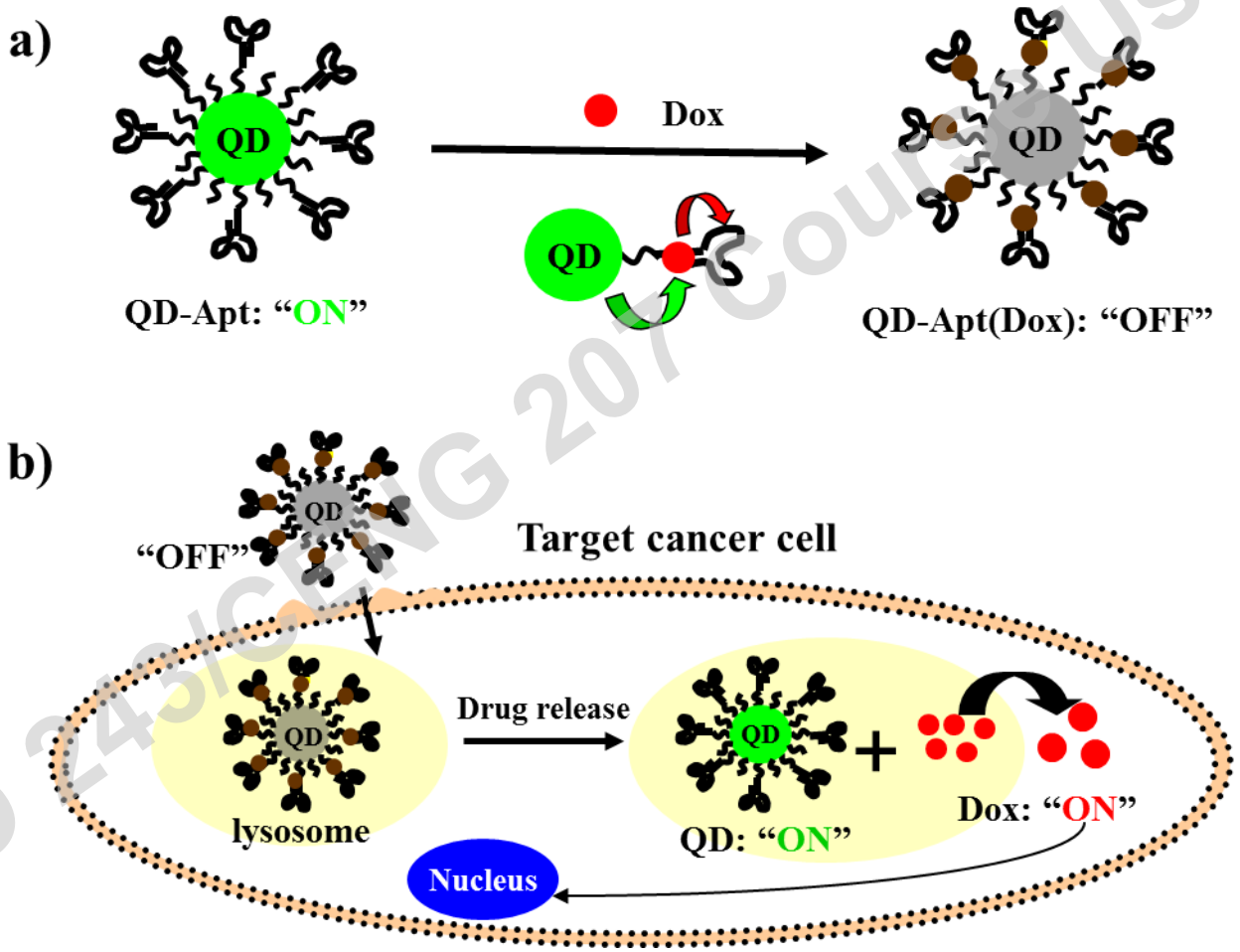

Nano Letters **2007**, *7*, 3065

Dox Quenches QD

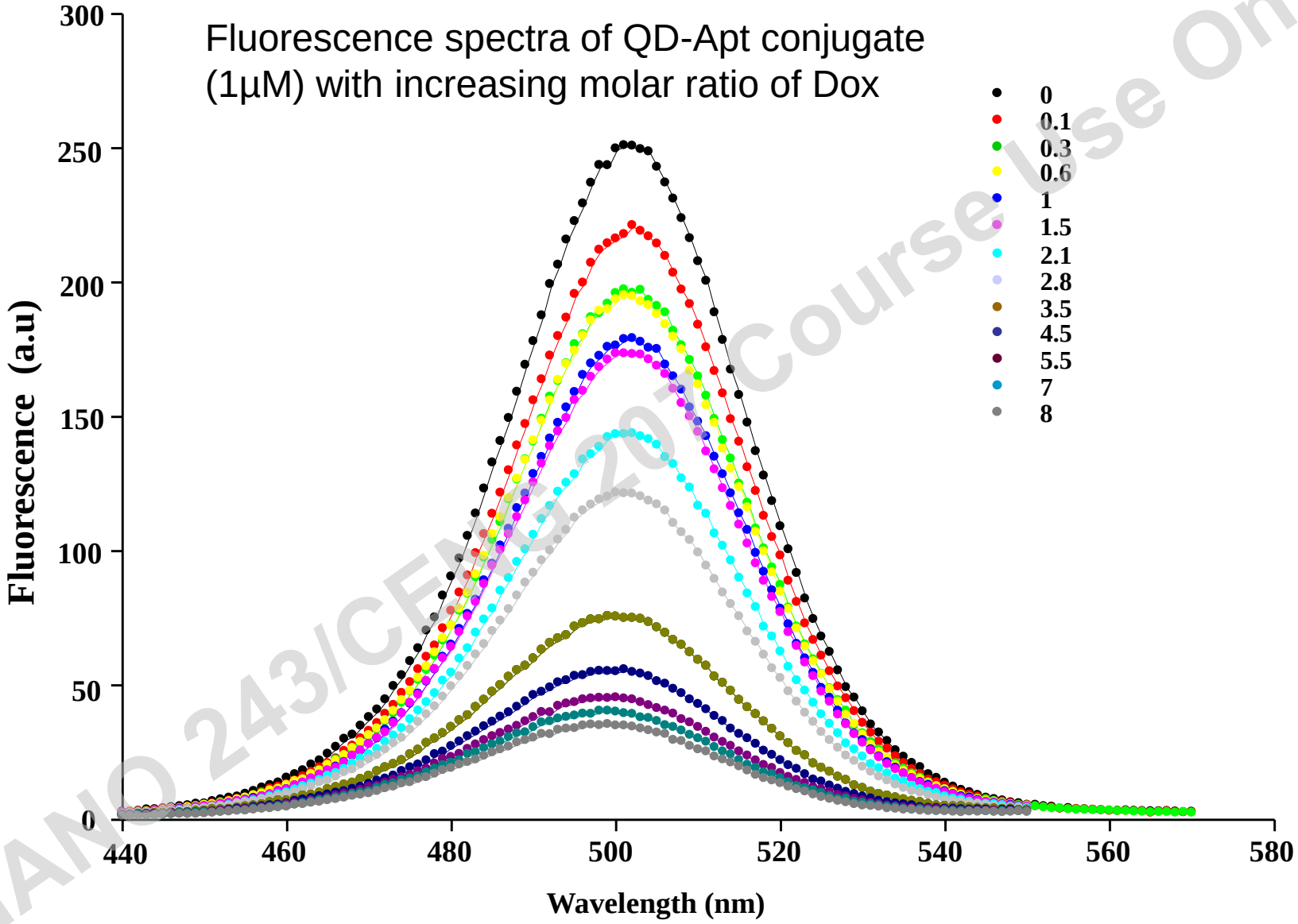

Aptamer Quenches Dox

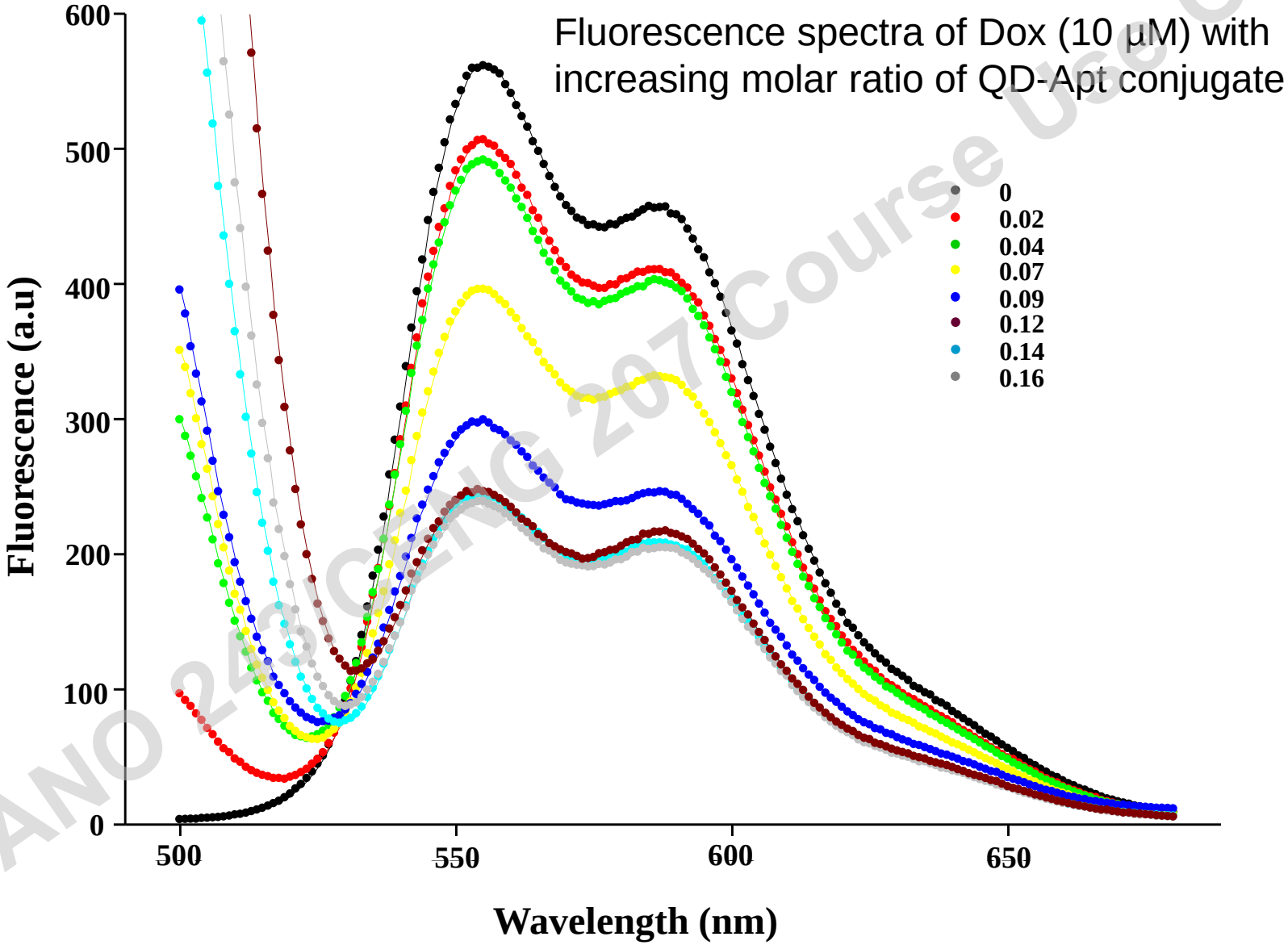

Aptamer-QD Conjugation

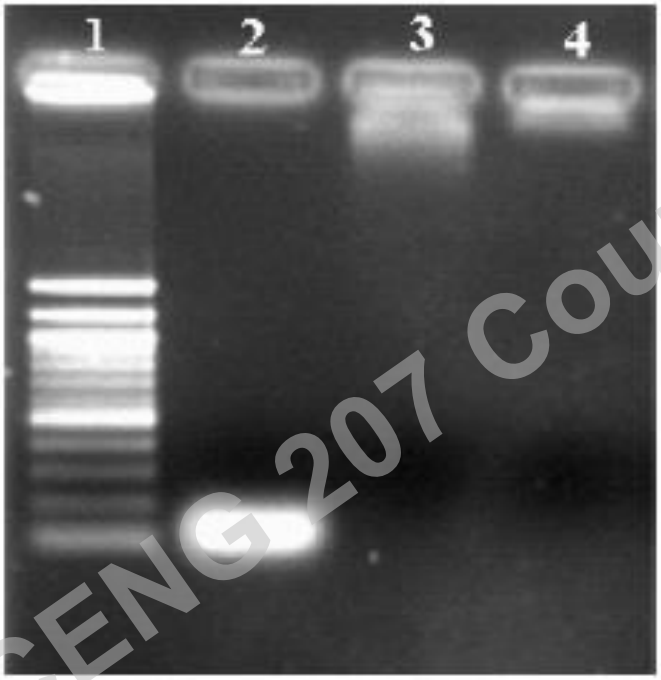

Gel electrophoresis results of QD-Apt conjugate after staining with ethidium bromide. Lanes 1, 2, 3, and 4 represent the 100 bp DNA ladder, A10 PSMA aptamer, QD-Apt conjugate, and QD alone, respectively.

Targeted Delivery

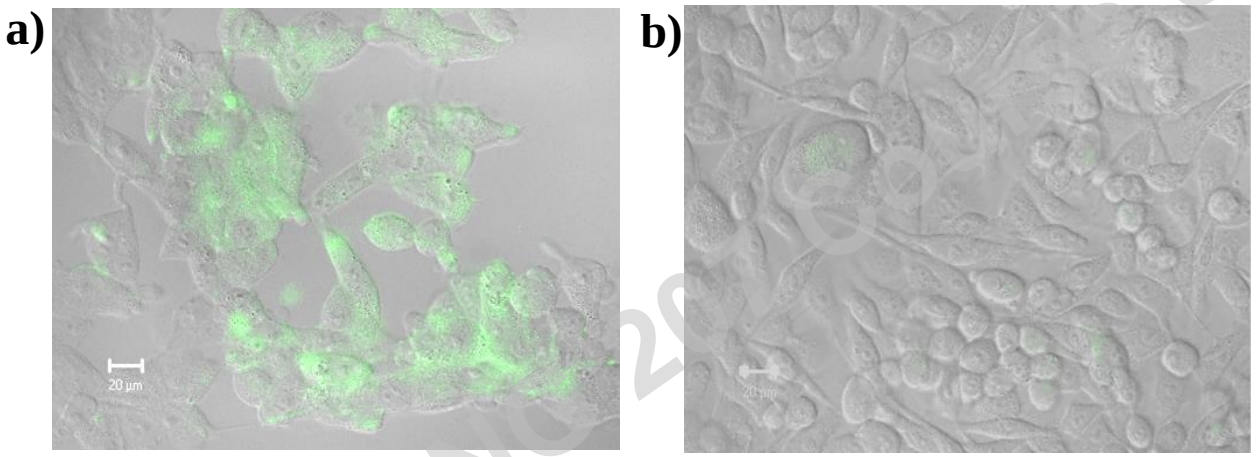

Binding of QD-Apt conjugates to (a) LNCaP (PSMA+), and (b) PC3 (PSMA-) prostate adenocarcinoma cells. QD is shown in green.

Imaging and Sensing of Drug Delivery

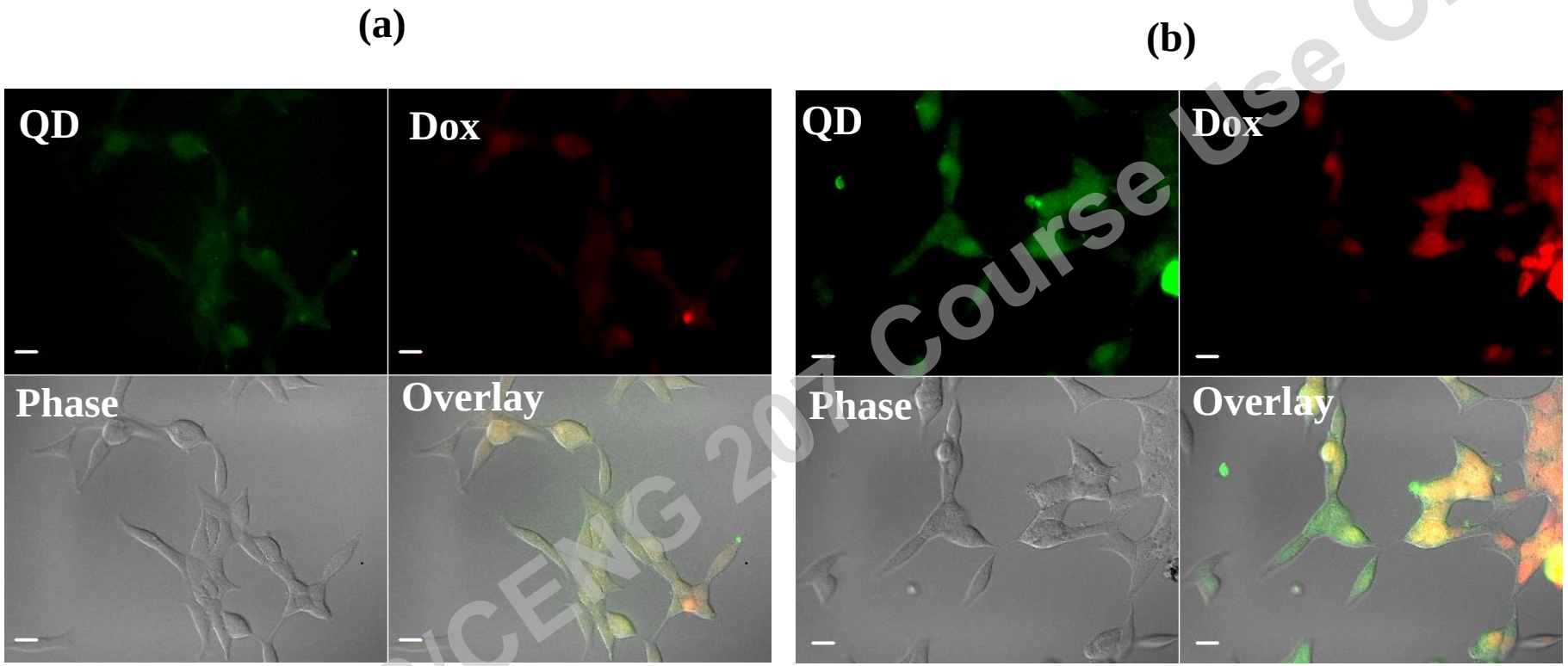

Confocal laser scanning microscopy images of PSMA expressing LNCaP cells after incubation with 100 nM QD-Apt-(Dox) conjugates for 0.5 h at 37 °C, washed two times with PBS buffer, and further incubated at 37 °C for (a) 0 h and (b) 1.5 h. Dox and QD are shown in red and green, respectively, and the lower right images of each panel represents the overlay of Dox and QD fluorescent.

In Vitro Therapeutic Efficacy (MTT assay)

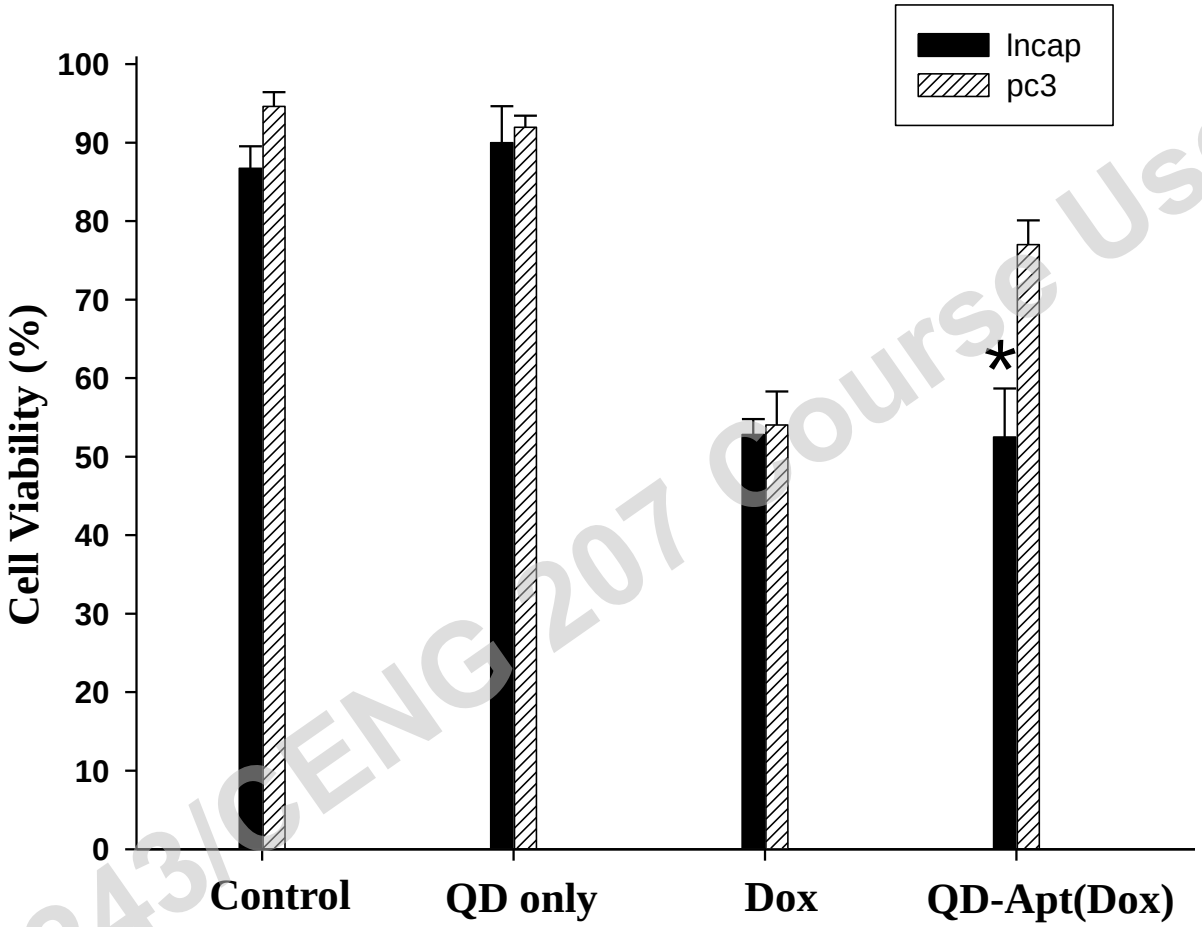

Prostate cancer cell lines, LNCaP (PSMA+) and PC3 (PSMA-), were incubated with QD alone (1.6 *í*M), Dox along (5 *í*M), or QD-Apt(Dox) conjugates (1.6 *í*M), for 3 h, and the cells were washed and further incubated for 24 h prior to measurement of cell viability.

Theranostics – Example 2

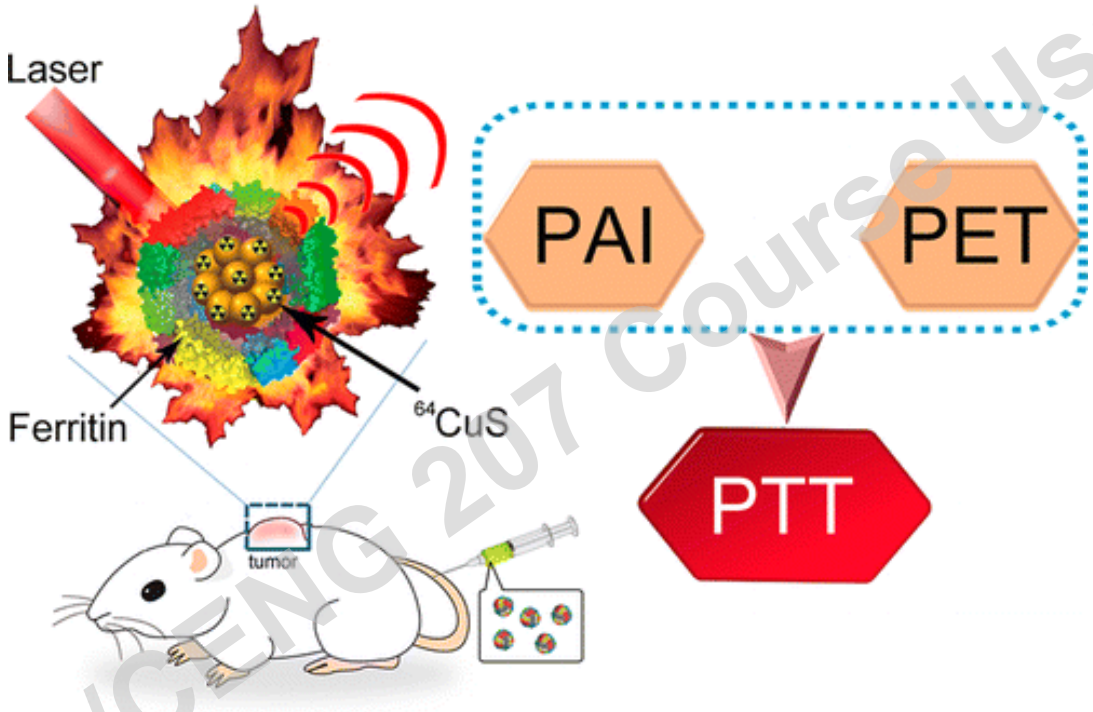

Copper Sulfide–Ferritin Nanocages (CuS–Fn NCs) as Clinically Translatable Cancer Theranostics for Positron Emission Tomography (PET) and Photoacoustic Dual-Modal Imaging (PET/PAI) Guided Photothermal Therapy (PTT)

ACS Nano **2016**, *10*, 3453

Copper Sulfide-Ferritin Nanocages (CuS-Fn NCs)

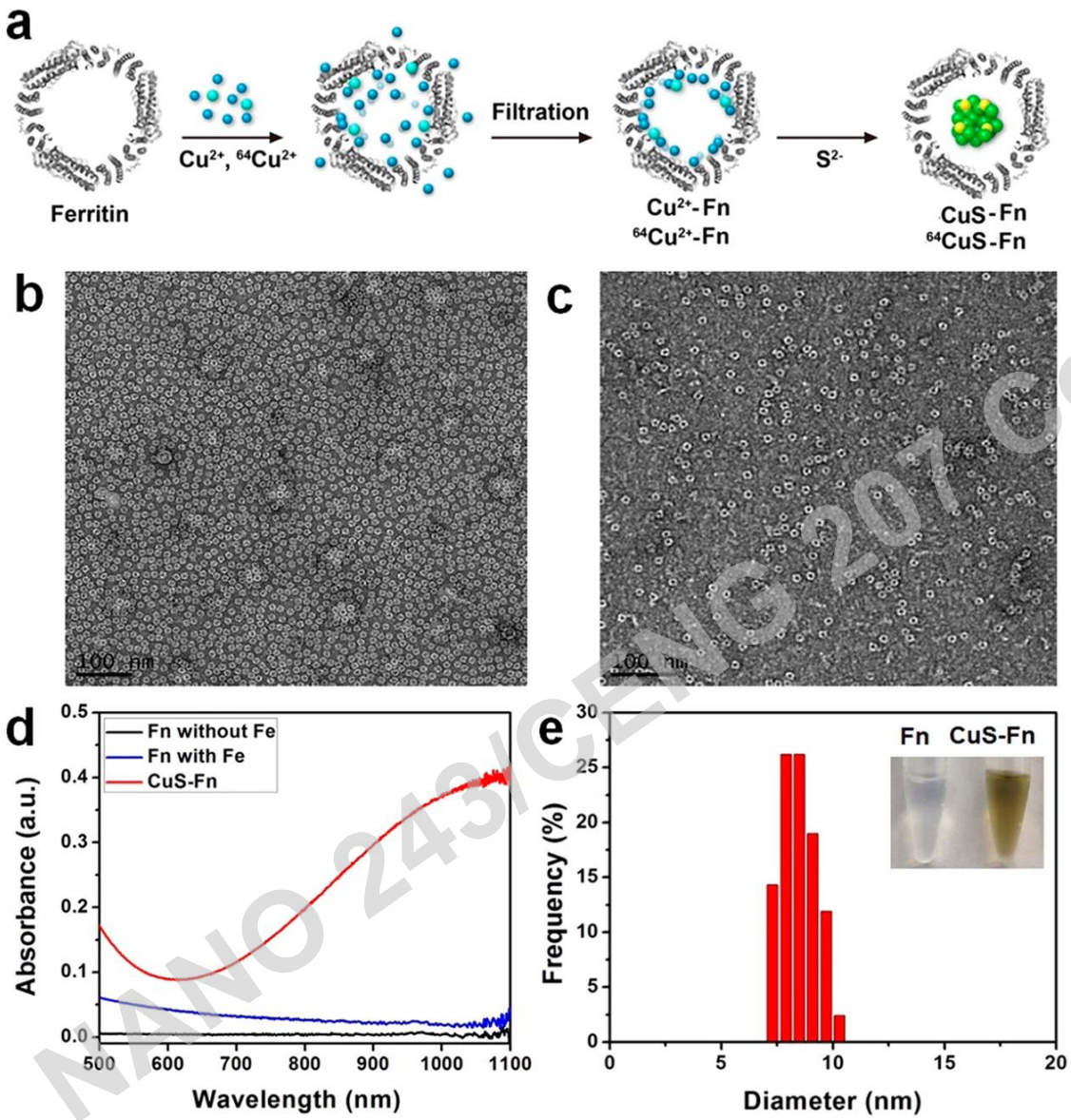

(a) The synthetic procedure of CuS–Fn NCs. (b) Representative TEM image of iron free Fn stained with 1% uranyl acetate. (c) TEM image of CuS–Fn NCs stained with 1% uranyl acetate. A clear dark CuS core can be seen inside the Fn cage. (d) UV–vis absorbance spectrum of Fn without iron, Fn and CuS–Fn NCs. (e) The size distribution of CuS core. Inset: The photograph of Fn and CuS–Fn NPs solutions.

Photothermal and Photoacoustic Properties

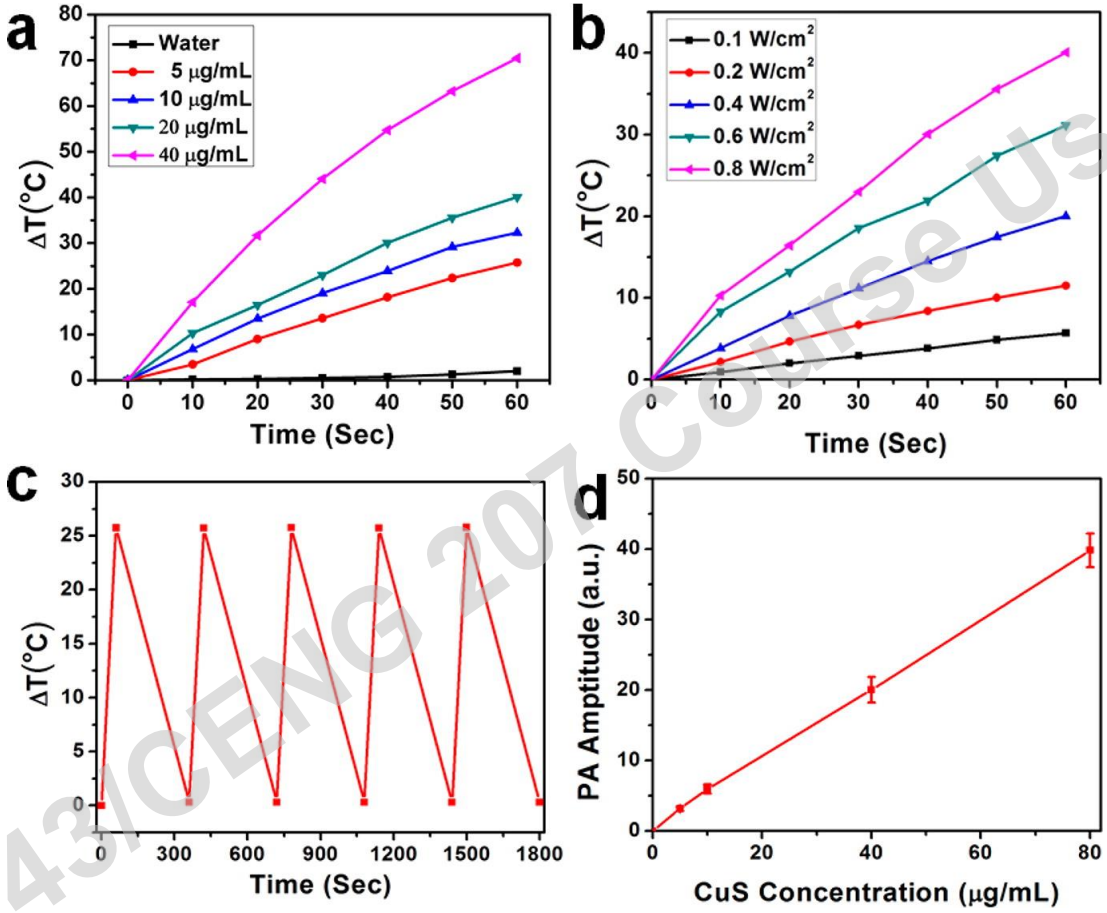

(a) Temperature rise after 60 s laser irradiation of different concentrations of CuS–Fn NCs and pure water. (b) Temperature rise after 60 s laser irradiation for CuS–Fn NCs solutions (20 μg/mL) of different laser powers. (c) Photothermal stability study of CuS–Fn NCs solution. (d) Photoacoustic signal amplification for CuS–Fn NCs of different concentrations.

In Vitro Cell Experiments

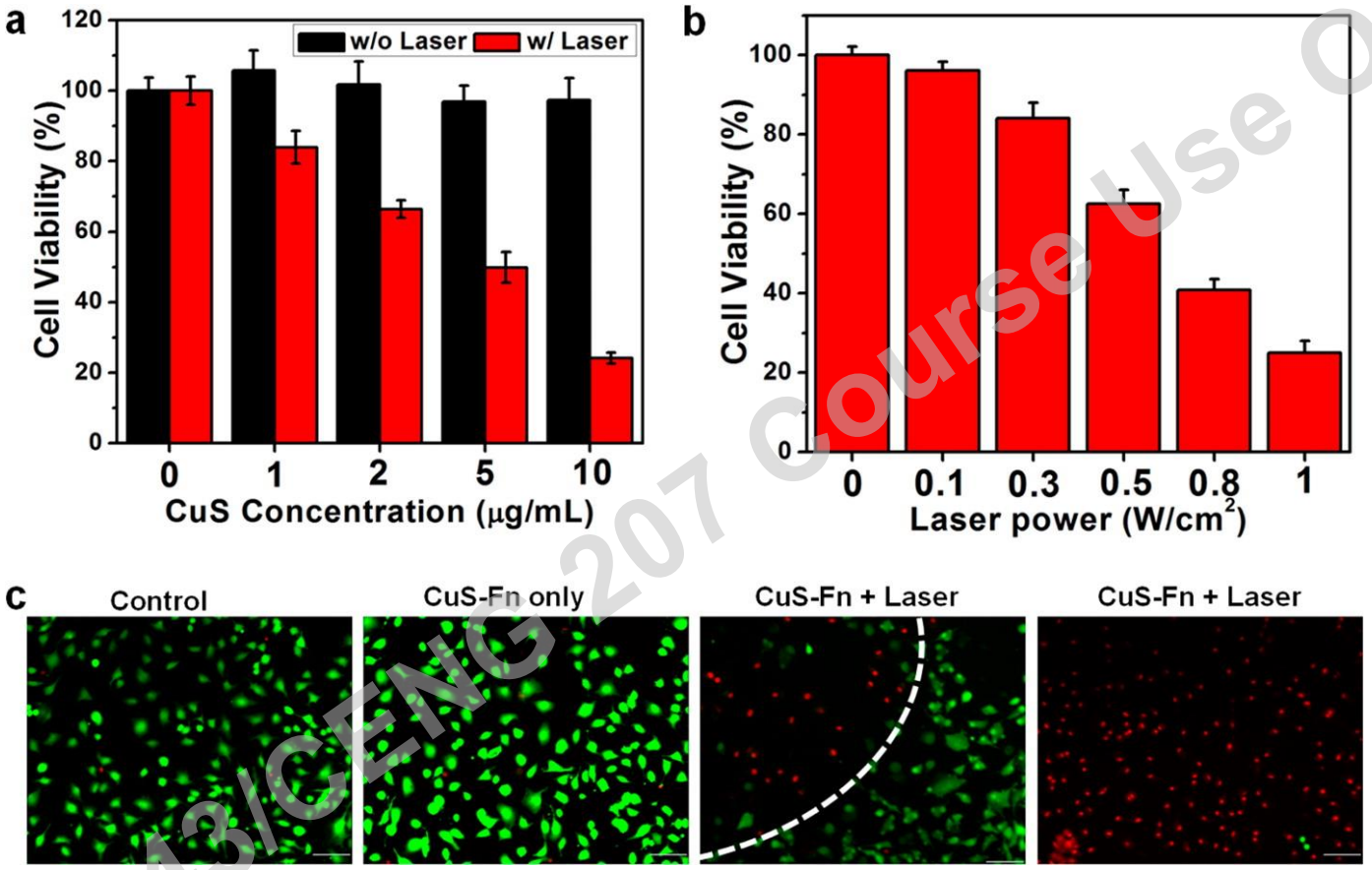

(a) Relative viability of cells incubated with gradient CuS–Fn NCs concentrations with or without irradiation by 808 nm laser. (b) Relative viability of U87MG cells incubated with 10 μg/mL CuS–Fn NCs after irradiation by 808 nm laser. (c) Fluorescence images of calcein AM/PI stained U87 MG cells after 4 h incubation with fresh medium, CuS–Fn NCs, and CuS–Fn NCs exposed to 808 nm laser. A clear laser spot can be seen in the irradiated CuS–Fn NCs group. Scale bar 100 μm.

In Vitro Tumor Experiments

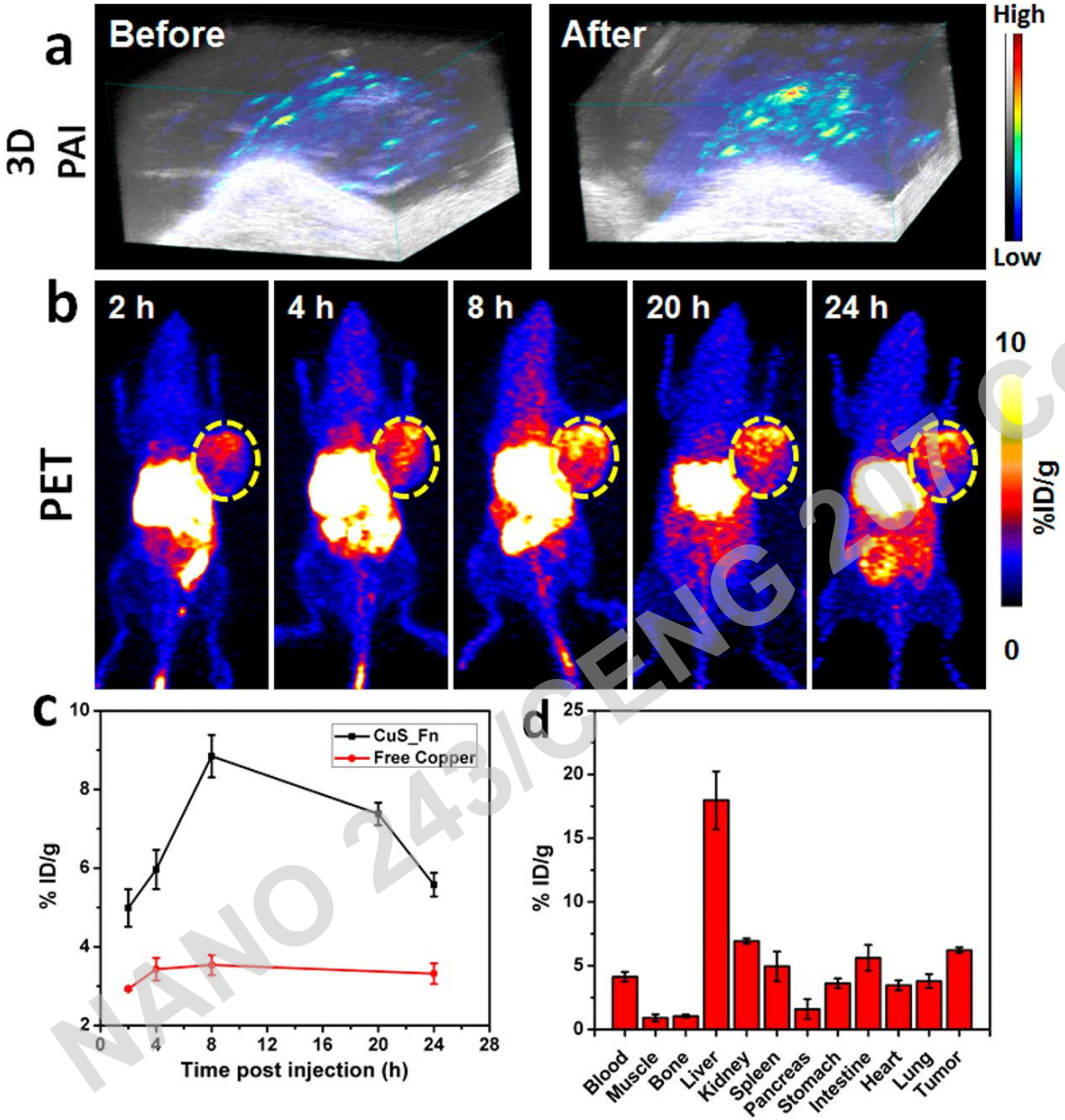

Photoacoustic and PET imaging of CuS–Fn NCs. (a) 3D Photoacoustic images of human glioblastoma U87MG tumor pre- and post-CuS–Fn injection. (b) PET images of tumor bearing mice 2, 4, 8, 20, and 24 h after iv injection of 50 μCi ^{64}CuS–Fn NCs. (c) Comparison of time-dependent tumor uptake between ^{64}CuS–Fn NCs and free copper groups. (d) Biodistribution of tumor and primary organs at 24 h time point.

Photothermal Therapy Efficacy

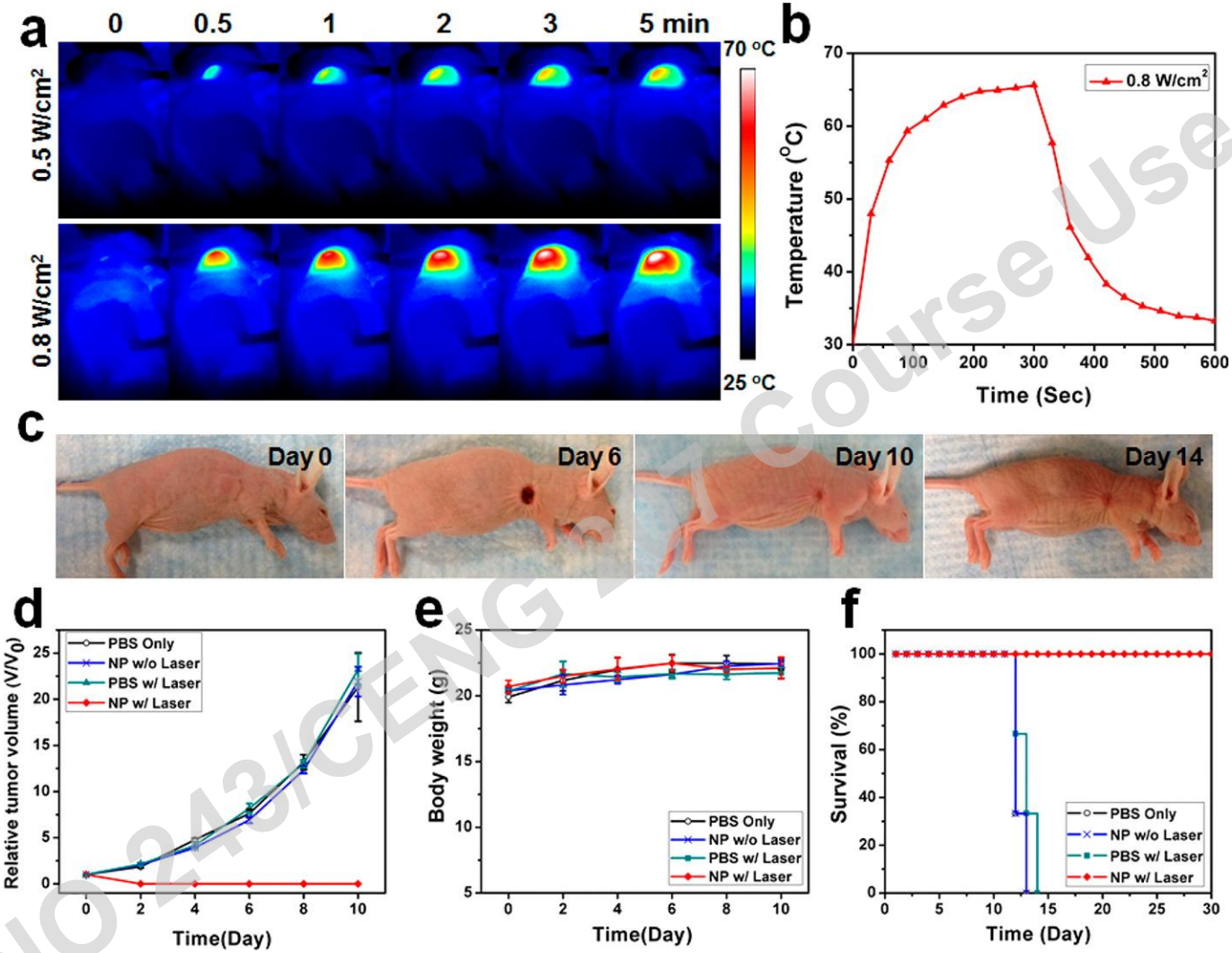

(a) Temperature recording of U87 MG tumor mice upon 5 min laser exposure of different powers. (b) Temperature change of tumor area upon laser irradiation. (c) Representative photos of U87MG tumor mice at different days after treatment. Tumor volume (d), body weight (e), and mice survival rate (f) curves of different groups of tumor-bearing mice after treatment.